Emissions of biogenic volatile organic compounds and subsequent photochemical production of secondary organic aerosol in mesocosm studies of temperate and tropical plant species

Kevin P. Wyche[1,2], Annette C. Ryan[3*], C. Nicholas Hewitt[3], M. Rami Alfarra[4,5], Gordon McFiggans[4], Timo Carr[1], Paul S. Monks[1], Kirsty L. Smallbone[2], Gerard Capes[5], Jacqueline F. Hamilton[6], Thomas A. M. Pugh[7], and A. Robert MacKenzie[8]

1. Department of Chemistry, University of Leicester, Leicester, LE1 7RH, UK

2. School of Environment and Technology, University of Brighton, Brighton, BN2 4GJ

3. Lancaster Environment Centre, Lancaster University, Lancaster, LA1 4YQ, UK

4. School of Earth, Atmospheric and Environmental Sciences, The University of Manchester, M13 9PL, UK

5. National Centre for Atmospheric Science, The University of Manchester, M13 9PL, UK

6. Dept. of Chemistry, University of York, York, YO10 5DD, UK

7. Karlsruhe Institute of Technology, IMK-IFU, Garmisch-Partenkirchen, Germany

8. Birmingham Institute of Forest Research, University of Birmingham, B15 2TT, UK

*For correspondence:
A. C. Ryan,
Lancaster Environment Centre,
Lancaster University,
Lancaster,
LA1 4YQ,
UK.

Tel: 01524 594 534
Email: a.ryan@lancaster.ac.uk

Abstract: Silver birch (*Betula pendula*) and three Southeast Asian tropical plant species (*Ficus cyathistipula, Ficus benjamina* and *Caryota millis*) from the pantropical fig and palm genera were grown in a purpose-built and environment-controlled whole-tree chamber. The volatile organic compounds emitted from these trees were characterised and fed into a linked photochemical reaction chamber where they underwent photooxidation under a range of controlled conditions (RH ~ 65 – 89 %, VOC/NO_x ~ 3 – 9 and NO_x ~ 2 ppbV). Both the gas phase and the aerosol phase of the reaction chamber were monitored in detail using a comprehensive suite of on-line and off-line, chemical and physical measurement techniques.

Silver birch was found to be a high monoterpene and sesquiterpene, but low isoprene emitter, and its emissions were observed to produce measureable amounts of SOA via both nucleation and condensation onto pre-existing seed aerosol (Y_{SOA} 26 – 39 %). In contrast, all three tropical species were found to be high isoprene emitters with trace emissions of monoterpenes and sesquiterpenes. In tropical plant experiments without seed aerosol there was no measurable SOA nucleation, but aerosol mass was shown to increase when seed aerosol was present. Although principally isoprene emitting, the aerosol mass produced from tropical fig was mostly consistent (i.e., in 78 out of 120 aerosol mass calculations using plausible parameter sets of various precursor specific yields) with condensation of photooxidation products of the minor VOCs co-emitted; no significant aerosol yield from condensation of isoprene oxidation products was required in the interpretations of the experimental results. This finding is in line with previous reports of organic aerosol loadings consistent with production from minor biogenic VOCs co-emitted with isoprene in principally-isoprene emitting landscapes in Southeast Asia. Moreover, in general the amount of aerosol mass produced from the emissions of the principally-isoprene-emitting plants, was less than would be expected from published single-VOC experiments, if co-emitted species were solely responsible for the final SOA mass. Interpretation of the results obtained from the fig data sets, leaves room for a potential role for isoprene in inhibiting SOA formation under certain ambient atmospheric conditions, although instrumental and experimental constraints impose a level of caution in the interpretation of the results.

Concomitant gas and aerosol phase composition measurements also provide a detailed overview of numerous key oxidation mechanisms at work within the systems studied and their combined analysis provides insight into the nature of the SOA formed.

Keywords: Secondary organic aerosol, biogenic volatile organic compounds, BVOC, gas-aerosol partitioning, isoprene, monoterpenes, mesocosm

Introduction

Atmospheric aerosols change the radiative balance of the Earth through scattering and absorbing incident solar radiation (Kim and Ramanathan, 2008); they directly and indirectly affect the properties and formation of clouds, thus altering the hydrological cycle (Gunthe et al., 2009;Junkermann et al., 2009;Stevens and Feingold, 2009); and they may have an impact on the efficiency of plant photosynthesis (Mercado et al., 2009), thereby modifying the uptake of atmospheric carbon. Hence, aerosol particles affect the Earth's climate in several ways (as reviewed in Hallquist et al., 2009;IPCC, 2007;Isaksen et al., 2009;Carslaw et al., 2010) as well as having a detrimental impact on human health (e.g., Baltensperger et al., 2008).

A large fraction of the observed atmospheric aerosol composition is organic (Zhang et al., 2007). A primary organic component is emitted directly into the atmosphere from anthropogenic activities, such as biomass burning and fossil fuel combustion, or is emitted from natural sources, such as plant abrasion and the sea surface. Secondary aerosol particles are formed within the atmosphere by gas-to-particle conversion; those formed from gas-phase organic precursors are known as secondary organic aerosol (SOA) (e.g., Riipinen et al., 2012). There is considerable uncertainty surrounding the chemical transformation of anthropogenic and biogenic volatile organic compounds (AVOC and BVOC, respectively) from the gas phase to the aerosol phase and hence, considerable uncertainty in the global source of SOA (Hallquist et al., 2009;Donahue et al., 2009;Ng et al., 2006;Virtanen et al., 2010).

On a global scale, approximately 90 % of all volatile organic compound emissions originate from biogenic sources (Guenther et al. 2012), with almost half of this being emitted from tropical and subtropical forests. The ability of biogenic VOC to form SOA is therefore of particular interest and potential importance. Globally, isoprene (2-methyl-1,3-butadiene, C_5H_8) is the biogenic VOC with the largest mass emission rate. It is estimated to account for about 50 % of BVOC emissions by mass (Guenther, et al. 2012), but it is still uncertain how much it contributes to SOA formation (Karl et al., 2009;Carlton et al., 2009).

Modelling, laboratory chamber experiments and field studies provide a range of possible yields of SOA from isoprene, typically of the order 0.1 – 3 % by mass, with some values reported as high as 5.5 % (van Donkelaar et al., 2007;Kleindienst et al., 2009, 2007;Kroll et al., 2005, 2006;Claeys et al., 2004a;Edney et al., 2005; Brégonzio-Rozier et al., 2014). SOA yields from the further oxidation of first and subsequent generation isoprene oxidation products, such as methacrolein, are estimated to be as much as 15 % (Rollins et al., 2009;Carlton et al., 2009;Claeys et al., 2004b;Robinson et al., 2010). Recent work has highlighted that under low NO_x conditions, SOA mass formed from isoprene oxidation could be influenced by the acidity of pre-existing aerosol via the reactive uptake of certain key isoprene oxidation products, namely isoprene epoxydiols (IEPOX; Surratt et al., 2010; Lin et al., 2012). More recently, Nguyen et al. (2014) found that the "pH dependence for OA formation from IEPOX was weak for AS particles". There is further evidence from chamber studies using temperate tree species such as birch, spruce and pine that isoprene may in fact suppress SOA formation from other VOC precursors, when present when present (Kiendler-Scharr et al., 2009a;Kanawade et al., 2011). It should be noted at this point that it is unclear in most cases how wall effects have been considered in the production of such yield values and whether the treatments employed are adequate such that the yields are comparable between chambers, or indeed between experiments.

Here, we characterised the BVOC emissions from three south-east Asian tropical plant species (*Ficus cyathistipula, Ficus benjamina* and *Caryota millis*) and in a series of coupled plant growth chamber–atmospheric reaction chamber experiments, we examined the ability of their oxidation products to contribute to SOA formation under atmospherically relevant conditions. In order to provide a geographically and chemically contrasting study, we replicated these experiments using common silver birch (*Betula pendula*). Silver birch has previously been shown to contribute to the formation of secondary organic aerosol via the emissions of mono- and sesquiterpenes (e.g. Kiendler-Scharr et al., 2009a;2009b;Mentel et al., 2009). Seeded (ammonium sulphate) and un-seeded experiments were carried out to allow studies of both fresh nucleation and condensation onto pre-existing aerosol.

Methods and materials

2.1 Plant selection and pre-screening

Three non-clonal specimens of common silver birch (*Betula pendula*), a monoterpene and isoprene emitting tree species; two species of fig (*Ficus benjamina* and *Ficus cyathistipula*), and one species of palm (*Caryota millis*), each approximately 1.5 m in height were used. Figs and palms are abundant in all tropical rainforests. We chose three species found in abundance throughout south and southeast Asia to be consistent with our field work (Hewitt et al., 2010a;MacKenzie et al., 2011). *Ficus benjamina* (Moraceae) is native to Malaysia and has previously been found to be a high isoprene emitter (0.03 – 8.7 μg C g^{-1} h^{-1}, potted and in soil) with emissions of the monoterpenes, limonene (0.02 μg C g^{-1} h^{-1}) and β-ocimene (1.8 – 2.5 μg C g^{-1} h^{-1}), and the sesquiterpenes β-caryophyllene and α-copaene (Carvalho et al., 2005;Geron et al., 2006). In addition, emissions of benzaldehyde (0.53 μg C g^{-1} h^{-1}) and acetaldehyde (69 μg C g^{-1} h^{-1}) from potted specimens have been detected (Carvalho et al., 2005). No previous data are available on the BVOC emissions from *Ficus cyathistipula* or *Caryota millis*. Proton transfer-reaction mass spectrometry (PTR-MS) and gas chromatography–mass spectrometry (GC-MS) screening, prior to the start of the coupled chamber experiments, confirmed that both species were high isoprene emitters with *Ficus cyathistipula* also emitting limonene, β-phellandrene, α-damascone and acetaldehyde. Analytical methods are described in detail in section 2.4.

2.2 Plant chamber design

A 4.7 m^3 plant chamber was constructed out of two rectangular Teflon bag sections and a Teflon lid (0.05 mm FEP) (Adtech Polymer Engineering, UK), which were each supported by frames built using 25 mm^2 box aluminium (Speed Frame, RS Components, UK). The framework stood on a raised foil and Teflon covered marine plywood base. PVC foam strips (RS Components, UK) ensured an airtight seal between chamber sections. Heavy-duty double-sided tape (RS components, UK) was used to secure the Teflon bags to the frame. The interior of the plant chamber was only exposed to Teflon surfaces.

Compressed air was constantly supplied to the plant chamber via a mass flow controller and regulator (ALICAT MCR-500 SLPM-D, Premier Control Technologies Ltd, UK) at 780 L min^{-1} and 7.5 bar via a 12.7 mm (outer diameter- OD) reinforced tube. This was reduced to approx 1 bar and between 250 to 300 L min^{-1} (+/- 0.8 %) dependent on the photosynthetic and transpiration rate of each plant species (equivalent to one complete air change every 15 - 20 mins). The air stream was passed through a 12.7 mm (OD) PTFE tube to three in-series filters to remove any pre-existing VOCs (activated carbon filter P3KFA14ASMN, Parker Pneumatic, UK), and submicrometer particles (HEPA CAP 75 filter capsule (FDP-780-050K, Fisher Scientific, UK)), and NO_x (Purafil and activated charcoal, Purafil Inc. USA). Finally, the air was re-humidified by passing it through a 2 L Teflon barrel (Jencons, UK) filled with warmed distilled water. The plant chamber outlet air was either vented into the laboratory via a 50 mm (OD) stainless steel pipe and valve, or used to fill an 18 m^3 Teflon reaction chamber.

To enhance mixing, air entered the plant chamber via a perforated 12.7 mm (OD) PTFE tube that circled the base of the chamber. One 12.7 mm stainless steel bulkhead fitting (Swagelok, UK) was inserted through the frame to secure the PTFE tube to the base of the plant chamber. A 50 mm (OD) stainless steel pipe was inserted into the upper corner of the chamber and supported by a Teflon (inner surface) and Nylon (outer surface) manifold (Plastics Direct, UK). The manifold also supported an EGM probe (EGM-4, PP Systems, UK), which recorded relative humidity (RH), temperature (T), CO_2 and photosynthetically active radiation (PAR).

Plants were kept in 255 – 330 mm (height) pots depending on species, watered to pot dripping point and sprayed twice weekly. Plant chamber conditions were maintained at 31 – 33.5 °C / 22 – 24 °C (day/night), 29 – 40 % / 33 – 44 % (day/night) RH, and 335 – 385 ppmV / 390 – 404 ppmV (day/night) CO_2. Owing to structural restrictions, PAR could not be measured directly under the growth lamps in the centre of the canopy. At the top edge of the canopy it was 500 µmol m^{-2} s^{-1} with a 12 hr day / night cycle.

2.3 Reaction chamber description

The aerosol photochemical reaction chamber at the University of Manchester is composed of an 18 m^3 FEP Teflon bag mounted on three rectangular extruded aluminium frames (Alfarra et al., 2012). A bank of halogen lamps and a 6 kW Xenon arc lamp are mounted on the enclosure housing the bag, which is coated with reflective “space blanket” providing an integrating sphere, maximising the irradiance in the bag and ensuring even illumination for the production of photochemical species such as the hydroxyl radical (OH). The air introduced to the bag is dried and filtered for gaseous impurities and particles, prior to humidification with high purity deionised water. A high capacity O_3 generator provides controlled ambient levels of O_3 (used as an oxidant) and high O_3 concentrations (serving as a cleaning agent between experiments).

Size-dependent (diffusional and gravitational) wall-loss rate constants were calculated based on particle mobility and the surface-to-volume ratio of the chamber (Verheggen and Mozurkewich, 2006). The diffusional loss rate uses a constant of proportionality, which can only be determined empirically. A time period was selected near the end of each experiment where the wall losses were deemed to be the dominant process affecting the size distribution. The volume size distribution at the beginning of this period had the calculated wall loss rate applied to simulate the evolution of the size distribution over the selected time period. If the calculated loss rate loss rate didn't reproduce the measured volume evolution within the specified tolerance (1 – 2 % in this work), the constant of proportionality for diffusional losses was adjusted such that the simulated volume at the end of the selected period matched the measured volume within the specified tolerance. The time-integrated gravitational and (optimised) diffusional loss rate constants were then applied to the volume size distribution throughout the experiment in order to reconstruct a wall loss corrected size distribution, which was then used to calculate the wall-loss-corrected particle mass.

Both the plant chamber and reaction chamber were tested for contaminants separately and when joined together by running the system with an empty plant chamber and by carrying out a “blank” run prior to each set of experiments.

2.4 Analytical techniques

2.4.1 Gas phase measurements

The volatile and semi-volatile organic compounds and oxygenated volatile organic compounds in both the plant chamber and the reaction chamber were measured by soft-ionisation mass spectrometry (PTR-MS, CIR-TOF-MS, described below) and gas chromatography-mass spectrometry (GC-MS).

The proton-transfer-reaction mass spectrometry (PTR-MS) instrument employed (Ionicon, Austria) comprises two turbomolecular pumps, a heated silica steel inlet system and a 9.6 cm long stainless steel drift tube. The nominal response time is approximately 1 s. The operating parameters of the PTR-MS were held constant during measurements, except for the secondary electron multiplier voltage, which was optimised each day. The drift tube pressure, temperature and voltage were 2.2 hPa, 50 °C, and 600 V, respectively. The central reaction chamber of the drift cell was operated at an *E/N* (*i.e.* electric field/gas number density) of 125 Td. The count rate of $H_3O^+.H_2O$ ions was 1 – 2 % of the count rate of H_3O^+ ions. The PTR-MS sampled continuously with a flow rate of 100 – 150 ml min^{-1} through 3.2 mm PTFE tubing.

The chemical-ionisation-reaction time-of-flight mass spectrometer (CIR-TOF-MS) comprises a temperature controlled (40 (±1) ^{o}C) ion-source drift cell assembly coupled to an orthogonal time-of-flight mass spectrometer equipped with a reflectron array (Kore Technology Ltd, Ely, UK). The ion-source deployed was a hollow cathode discharge type (Blake et al., 2009) and the chemical ionization technique used was proton transfer reaction from hydrated hydronium ($H_3O^+.H_2O$) (Jenkin et al., 2012). Sample air was delivered in a continuous stream directly to the drift cell via a 0.5 m long, 6.35 mm (internal diameter) Teflon sample line, heated to 40 (±1) ^{o}C, at a constant flow rate of 80 ml min^{-1}. The central reaction chamber of the drift cell was operated at an *E/N* ratio of ~ 90 – 100 Td, with a tuned energy ramp at the base of the cell to remove potential water-cluster ions (e.g. $RH^+.H_2O$). Further information regarding the CIR-TOF-MS design and a detailed discussion regarding its operation can be found in Blake et al. (2004) and Wyche et al. (2007).

The PTR-MS and CIR-TOF-MS were calibrated using three different methods: (i) step-wise dilution of a gravimetrically prepared gas standard (BOC Special Gases, UK) containing a variety of VOCs and OVOCs; (ii) using calibration material produced in-house via the injection of liquid samples into 10 l Tedlar bags (SKC Inc., USA) containing either humidified or dry, pure nitrogen; and (iii) using gas standards derived from permeation tubes (Vici Inc., US; Ecoscientific, UK), diluted, humidified and delivered by a commercial calibration unit (Kintec, model: 491). Where experimental calibration was not possible for a specific compound, either the calibration sensitivity for a structurally similar surrogate was used or calculated concentrations were employed (Jenkin et al., 2012). For the quantification of isobaric signals, a single sensitivity value was used, e.g. α-pinene sensitivity for Σ(monoterpenes) and β-caryophyllene sensitivity for Σ(sesquiterpenes); again working on the principal that structurally similar compounds possess similar PTR and CIR sensitivities.

CIR-TOF-MS and PTR-MS detection limits are reagent, reaction, analyte and sample matrix specific. However, typical CIR-TOF-MS detection limits, using PTR ionisation from hydronium, are of the order 0.4 ppbV $(10\ \text{min})^{-1}$ for more polar compounds, such as OVOCs (e.g. 2-hexanone) and as much as 10 ppbV min^{-1} for certain less polar compounds, such as smaller hydrocarbons (e.g. 1-pentene). For further details see Wyche et al., 2007.

The GC-MS system (GC-MS Turbomass Gold, Perkin Elmer, USA) comprised a thermal desorption autosampler (Perkin-Elmer ATD 400) connected via a heated (200 °C) transfer line to a Hewlett-Packard 5890 GC with a 5970 mass-selective detector. Compounds were desorbed at 280 °C for 5 min at 25 mL min^{-1} onto a Tenax-TA cold trap maintained at - 30 °C. The cold trap was then heated to 300 °C for 6 min to desorb compounds onto the GC column. Chromatographic separation was achieved using an Ultra-2 column (Agilent Technologies: 50 m × 0.2 mm ID × 0.11 μm film, 5 % phenylmethyl silica). An initial oven temperature of 35 °C was maintained for 2 min, and then increased at 4 °C min^{-1} to 160 °C followed by an increase of 45 °C min^{-1} to 300 °C, which was maintained for 10 min. The carrier gas was Helium supplied at a rate of 1 mL min^{-1}, with an injector temperature of 250 °C. The limit of detection for isoprene and monoterpenes was approximately 0.25 ng on column and 2 ng on column for sesquiterpenes, corresponding to 100 pptV of isoprene, 50 pptV of monoterpenes, and to 400 pptV of sesquiterpenes in a 1 L sample. Sampling was conducted by drawing 8 L of the analyte air through 6.35 mm PTFE tubing onto the GC-MS sample tubes using a handheld pocket pump (SKC Ltd, UK) at a flow rate of 150 ml min^{-1} (total sample time ~ 43 mins). Sample tubes were stored at 4 °C until analysed. VOC quantification was by comparison with commercially available liquid standards (Aldrich, Fluka and Sigma) diluted in methanol. Isoprene quantification was by comparison with a 700 ppbV in N_2 certified gas standard (BOC, UK).

NO and NO_2 mixing ratios were measured using a chemiluminescence gas analyser (Model 42i, Thermo Scientific, MA, USA). Ozone was measured using a UV photometric gas detector (Model 49C, Thermo Scientific, MA, USA).

2.4.2 Particle phase measurements

Within the main reaction chamber, a scanning mobility particle sizer (SMPS) system was used to measure the particle size distribution and total aerosol mass concentration (without sample drying). A particle density of 1.3 g cm^{-3} was assumed for calculating the mass of SOA particles in un-seeded experiments (Alfarra et al., 2006; Bahreini et al., 2005). For seeded experiments, a density of 1.77 g cm^{-3} was used to calculate the ammonium sulphate seed mass and 1.3 g cm^{-3} was assumed for calculating the additional SOA mass. A water-based condensation particle counter (wCPC, TSI

3786) was used to count the total particle number concentration between 2.5 nm and approximately 3 μm. Further instrument details can be found in Alfarra et al., 2012, and references therein.

Real-time broad chemical characterisation of the SOA was made using a compact Time-of-Flight Aerosol Mass Spectrometer (cToF-AMS, Aerodyne Research Inc., USA). A detailed description of the instrument, its operation and calibrations can be found elsewhere (Drewnick et al., 2005;Canagaratna et al., 2007). The instrument was operated in the standard configuration, taking both mass spectrum (MS) and particle-time-of-flight (PToF) data and was calibrated for ionisation efficiency using 350 nm monodisperse ammonium nitrate particles. The vapouriser was set at approximately 600 ^{o}C and data were collected at a time resolution of 2 min. A collection efficiency value of unity was applied to these data, based on evidence from a previous chamber study (Alfarra et al., 2006).

Filter samples for offline analysis were collected (without denuders) in a specially constructed holder, positioned in the chamber vent line. Aerosol samples were collected onto 47 mm quartz fibre filters (Whatman) at a rapid flow rate of 3 m^3 min^{-1} (sample time ca. 6 mins.). After sampling, filters were immediately placed in pre-cleaned glass vials and stored below -20 °C until analysis. The filter collection procedure employed here is much faster than traditional filter collection methods, which should minimise any potential negative and positive artefacts.

The filters were extracted into high purity water, filtered, evaporated to dryness and redissolved in 1 ml 50 % MeOH : 50 % H_2O. The water-soluble compounds were analysed using liquid chromatography-ion trap mass spectrometry (LC-MS/MS). Reverse phase LC separation was achieved using an HP 1100 LC system equipped with an Eclipse ODS-C_{18} column with 5 μm particle size (Agilent, 4.6 mm x 150 mm). Samples (60 μl) were injected then eluted by gradient elution with solvents A: 0.1% v/v formic acid water (Optima grade, Fisher) and B: methanol (Optima grade, Fisher) and a gradient program of 3 % B at time 0 min to 100 % B at 60 minutes with a flow rate of 0.6 ml min^{-1}. Mass spectrometry analysis was performed in negative ionisation mode using an HCT-Plus ion trap mass spectrometer with electrospray ionisation (Bruker Daltonics GmbH). Electrospray ionisation (ESI) was carried out at 350 °C with a nebuliser pressure of 4.82 bar and a nitrogen drying gas flow of 12 l min^{-1}. Further details can be found in Hamilton et al., 2013.

2.5 Experimental protocol

Three plants were placed in the plant chamber a minimum of 48 hours prior to the start of the experiment. Both the pots and soil were isolated by enclosing them in PFTE sheeting; this acted to prevent VOC emissions from the plastic pots and soil NO_x emissions from entering the chamber air. Three experiments were carried out on each species over a one-week period, after which the plants were removed and replaced with three plants of the next species, and the experiment cycle repeated.

Prior to each experiment, ozone was added to the chamber to give a mixing ratio of approximately 2 ppmV and was left overnight. The chamber was then filled and flushed several times using clean air from the facility's main inlet system (including Purafil, charcoal and HEPA filters as described above), until the total particle count (as measured by a water based condensation particle counter) was below 10 cm^{-3} and the O_3 and NO_x levels were less than 1 and 2 ppbV, respectively. At this point, the reaction chamber was flushed and then connected to the plant chamber for filling with the plant VOC emissions. Aerosol and gas phase composition and concentrations were continuously monitored throughout. At the end of the filling process, the plant chamber was disconnected from the reaction chamber, and within the space of roughly one minute, both the chamber lights were turned on and pure O_3 was injected to provide an initial concentration of around 20 or 70 ppbV (experiment dependent). The switching on of the chamber lights marked the start of each experiment, which typically lasted 6 hours from this point. For experiments using pre-existing seed, polydisperse ammonium sulphate particles (diameter between 40 – 60 nm) were generated from an aqueous solution using an aerosol nebuliser (Topas, ATM 230) and injected without drying into the reaction chamber at the end of the filling from the plant chamber.

In our experiments we chose to use ammonium sulphate for the aerosol seeds, rather than acidic particles that could otherwise promote isoprenoid particulate mass formation. Whilst it is recognised that isoprenoid SOA mass can be enhanced by the presence of acidic aerosol seed as originally reported by Jang et al. (2002) and subsequently by Limbeck et al. (2003), Edney et al. (2005), Kleindienst et al. (2007), Limbeck et al. (2007) and Surratt et al. (2007), we have limited our study to SOA formation in the mixed precursor systems without deliberate enhancement of particle mass by condensed phase reaction. There is clear evidence that isoprene oxidation can contribute to atmospheric SOA formation (e.g. Claeys et al., 2004, Edney et al., 2005) and we have previously found that enhancement in SOA from isoprene oxidation above the Bornean rainforest compared with the Amazon may result from an enhanced marine acidic sulphate contribution to sub-micron aerosol (Robinson et al., 2011). Intermediates in SOA formation from isoprene have been identified (e.g. Lin et al., 2012, 2013) and mechanisms for the acid catalysed formation proposed (Surratt et al., 2010). Whilst out of the scope of the current study, this should be the focus of future work.

Air samples were taken from three separate locations: 1) immediately before the plant chamber (pre-PC) for blank subtraction, 2) immediately after the plant chamber (post-PC) during the reaction chamber filling period for directly emitted BVOC and 3) from the reaction chamber (RC) during the experiment. RC air was monitored continuously using PTR-MS and CIR-TOF-MS for VOC decay and formation of reaction products. Air samples from the pre-PC and post-PC position, as well as RC air samples immediately at the start of each experiment and 1, 2, 4 and 6 hours after the lights were switched on, were collected on Tenax TA and Carbotrap filled stainless steel tubes (Supelco Inc, PA, USA) for GC-MS analysis.

Relative humidity (%), CO_2 (ppmV), PAR (μmol m^{-2} s^{-1}), and temperature (°C) in the plant chamber were recorded every 5 or 10 mins during reaction chamber filling, and every 15 or 20 mins overnight. System blanks were taken at the start and end of the experimental period. The reaction chamber background was checked and characterised through the performance of regular blank experiments (one in every five experiments). NO_x (NO, NO_2 and NO_3) and O_3 were continuously monitored in the reaction chamber. A list of all experiments and their general parameters is given in Table 1.

2.6 Calculated OH concentrations

Since isoprene losses are controlled by reaction with ozone and the hydroxyl radical (OH), the concentration of OH available to react with isoprene in the reaction chamber for each experiment was calculated based on the measured concentrations of O_3 and isoprene in each experiment, the rate of change in isoprene concentration, and the rate constants for the reactions of isoprene with OH and O_3, using equation (1):

$$\frac{\frac{d[Isoprene]}{dt} + k_{O_3}[O_3][Isoprene]}{-k_{OH}[Isoprene]} = [OH] \qquad \text{Eq}^{n}\ (1)$$

Hourly averaged concentrations of O_3 and isoprene were calculated for five of the experiments using the tropical fig. Using these data along with equation (1) a range of OH concentrations were obtained. For the first hour after lights on, [OH] was estimated to be 1.9 x 10^5 – 9.5 x 10^5 molecules cm^{-3}, whereas, towards the end of the experiment after roughly five hours, values of $8.1 \times 10^5 - 1.9 \times 10^6$ molecules cm^{-3} were obtained. In general, during the tropical fig experiments, [OH] estimated from isoprene and ozone was observed to steadily increase over the duration of the experiment from 0 – 5 hours after lights on.

2.7 VOC/NO$_x$ Conditions

Figure 1 shows the time-dependent mixing ratios of ozone and oxides of nitrogen for each experiment set. Although every effort was made to keep the concentrations of oxides of nitrogen low, measurable amounts were present, giving initial VOC/NO$_x$ ratios of the order 2 – 6 and 3 – 9 (see Table 1), for the birch and fig experiments, respectively (where here, the VOC concentration is equal to the sum of all potential precursor concentrations). In terms of a “Sillman plot” (Sillman, 1999), the experiments were carried out in the “VOC sensitive regime”.

The absolute concentration of VOCs in the reaction chamber was roughly ten times greater than those measured over the rainforest during our field experiments (Mackenzie et al., 2011) and the VOC/NO$_x$ ratios employed here were as much as ten times lower (i.e. typical ratio of 20:1, isoprene:NO$_x$ over the rainforest) (Hewitt et al., 2010b). The source of the NO$_x$ in the reaction chamber (initially ~ 2 – 6 ppbV NO$_x$, but increasing to ~ 5 – 9 ppbV after ~ 5 hours) is attributed to a small amount of diffusion of outside ambient air across the porous Teflon membrane into the reaction chamber. The production of certain reactive intermediates in the oxidation of VOCs (e.g., hydroxyl hydroperoxides from isoprene oxidation) is very sensitive to NO_x concentrations in the reaction mixture.

Results

3.1 Experiments with Betula pendula

3.1.1 Gas phase

Continuous gas phase monitoring with the CIR-TOF-MS and PTR-MS throughout the experiments, indicated successful transfer of VOC precursor material from the plant chamber to the reaction chamber prior to lights on. The data indicated that there was negligible loss of precursor compounds during the chamber transfer process (Fig. 2a).

Immediately after initiation of the photochemistry, the VOC precursor concentrations were observed to decay and product ions began to appear in the CIR and PTR mass spectra. Approximately sixty product-ion peaks were observed by the CIR-TOF-MS and the PTR-MS in the organic gas phase during a typical *Betula pendula* experiment. The temporal profiles of a number of the most abundant (O)VOCs measured are shown in Fig. 2. From a combination of the CIR-TOF-MS, PTR-MS and GC-MS observations (and from those observations discussed below for the tropical plant experiments), over fifty different hemi-, mono- and sesqui-terpene oxidation products were tentatively identified (Fig. 3 and Tables S1 – S5 in the supplementary information).

From initial inspection of the data, it is clear that monoterpenes dominate during the *Betula pendula* experiments (Fig. 2a and b), with strong signals observed in the CIR-TOF-MS and PTR-MS mass spectra at *m/z* 137 (protonated parent ion) and 81 (hydrocarbon fragment). A small amount of isoprene was also detected during *Betula pendula* experiments; however this was always significantly lower in magnitude than that of the sum of monoterpenes; for example, during the experiment on 07/07/09, 12.6 (± 3.8) ppbV monoterpenes were measured in the reaction chamber prior to lights on (c.f. 11.4 ppbV total monoterpenes measured at the post-PC position by the GC-MS), whereas only 2.0 (± 1.0) ppbV isoprene was detected. Speciation of the monoterpenes by GC-MS indicated that the most dominantly emitted C_{10} compounds from *Betula pendula* were α- and β-pinene (Table 2).

C_{15} sesquiterpenes (parent ion *m/z* 205) were detected in the plant and reaction chambers during each *Betula pendula* experiment, with the most abundant species identified by GC-MS being β-caryophyllene (Table 2). Sesquiterpenes were also measured in the reaction chamber by CIR-TOF-MS (Fig. 2c), however for the majority of the experiments they were present at concentrations either close to or below the detection limit, hence they could not always be monitored as a function of reaction time. For the experiment on 07/07/09, 1.7 (± 0.9) ppbV sesquiterpenes were measured by the CIR-TOF-MS prior to lights on (c.f. 2.2 ppbV total sesquiterpenes measured at the post-PC position by the GC-MS). An ion of *m/z* 153 was also observed in the PTR and CIR mass spectra of the plant chamber emissions and subsequently in the reaction chamber air, tentatively assigned (and here after referred to) as camphore.

During the reaction phase of the *Betula pendula* experiments the CIR-TOF-MS mass spectra were dominated by ions of relatively high mass (i.e. $m/z > 100$) pertaining to products of both monoterpene and sesquiterpene oxidation. The ions of highest mass (i.e. m/z 170 – 290) are characteristic of sesquiterpene oxidation, and have been observed recently during a similar chamber study investigating β-caryophyllene photo-oxidation (Jenkin et al., 2012). Drawing a comparison between these data and the detailed β-caryophyllene study conducted by Jenkin et al. (2012), a number of tentative assignments have been made for β-caryophyllene products, with the assumption that other precursor specific structural isomers may also occupy the same mass channels. A full list of example tentative assignments is given in the supplementary information (Table S2). In total the sum of all sesquiterpene products measured in the chamber was estimated to be ~ 1.5 ppbV (assuming an average PTR sensitivity for such high mass, oxygenated, compounds).

In contrast to the small amounts of sesquiterpene products observed in the reaction chamber, the products observed in greatest abundance were those derived from monoterpene decay. The largest (combined) product signal measured by the CIR-TOF-MS was that of $\Sigma(I_{111}, I_{93})$, where I_x is the intensity of the mass spectrum at $m/z = x$ (Fig. 2d). Previously, the m/z 111 and 93 signals have been shown to correspond to various primary C_7 unsaturated aldehydes formed during the oxidation of unsaturated acyclic monoterpenes, such as myrcene, ocimene and linalool (Lee et al., 2006a; Lee et al., 2006b; Ng et al., 2006; Wyche et al., In Preparation). In the case of myrcene and ocimene, the *m/z* 111 and 93 signals correspond to the parent ion (MH^+) and the dehydrated daughter fragment, respectively (MH^+-H_2O), and in the case of linalool *m/z* 111 corresponds to the dehydrated daughter ion and *m/z* 93 is a further fragment. The concomitant *m/z* 111 and 93 signals have also been reported to result from a C_7 cyclic ketone formed during the oxidation of terpinolene (not found in the *Ficus* emission profile and < 1 ppbV found in the *Betula* profile). The *m/z* 111 and 93 ions have previously been observed to be significant contributors to total ion signal in the PTR mass spectra during single precursor chamber experiments with concomitant SOA formation (Lee et al., 2006a; Lee et al., 2006b; Ng et al., 2006; Wyche et al., In Preparation), and the *m/z* 111 ion has also been observed in ambient air measurements over a forested region (Holtzinger et al., 2005).

As can be seen from observation of Fig. 2(d), the $\Sigma(I_{111}, I_{93})$ signal rises rapidly during the initial stages of the experiment, much more so than other monoterpene oxidation products (c.f. Fig. 2e), suggesting that the precursor has a much shorter lifetime with respect to OH and O_3. Of those monoterpenes speciated by the GC-MS, ocimene and linalool have the shortest lifetimes, with $k_{OH} = 3.04$ and 1.6×10^{-10} cm^3 molecule^{-1} s^{-1} (average lifetimes with respect to OH ~ 44 and 55 mins.), respectively, compared to $k_{OH} = 7.4 \times 10^{-11}$ cm^3 molecule^{-1} s^{-1} for β-pinene (average lifetime with respect to OH ~ 1458 mins.) (Atkinson and Arey, 2003; Kim et al., 2011). The $\Sigma(I_{111},$

I_{93}) signal peaks at around 60 – 100 mins at 3.0 (± 0.7) ppbV (concentration estimated using pinonaldehyde sensitivity), before decaying at a greater rate than that of the precursor monoterpenes and the other monoterpene products. This relatively short lifetime gives further insight into the potential identity of the *m/z* 111 and 93 signals, perhaps indicating the presence of multiple C=C bonds in the hydrocarbon structure, as would be found in the primary C_7 aldehydes obtained from the oxidation of ocimene or myrcene for example. Other short-lived biogenic oxidation products that could exist in such mesocosm systems, include α-hydroxy carbonyls, similarly formed following OH addition to a C=C bond.

Other dominant signals observed by the PTR-MS and CIR-TOF-MS during oxidation of the *Betula pendula* air matrix, include the sum of *m/z* 169 + 151 + 107, which respectively correspond to the parent ion and two daughter fragments of a number of primary monoterpene keto-aldehydes (which, from the speciated monoterpene plant chamber data, are most likely to be pinonaldehyde, caronaldehyde and α/γ-terpinaldehyde); and *m/z* 139, corresponding to the parent ion of a number of primary monoterpene ketones (most likely to be nopinone and caronone, again when considering the monoterpenes speciated by the GC-MS). As shown in Fig. 2(e) the primary keto-aldehyde and ketone signals had similar temporal profiles to one another, growing at a slower rate than that of $\Sigma(I_{111}, I_{93})$, to peak concentrations of around 0.9 (± 0.3) and 1.2 (± 0.3) ppbV, respectively, as the monoterpene trace tended towards zero. The temporal profile for the sum of all other "monoterpene like" product ions (i.e. ions of *m/z* > 90) was very similar to those of the primary keto-aldehyde(s) and ketone(s), peaking at a combined mixing ratio of approximately 3.5 ppbV (assuming an average PTR sensitivity for such high mass, oxygenated, compounds).

During the oxidation of compounds emitted by *Betula pendula*, the primary isoprene products, methyl vinyl ketone (MVK) and methacrolein (MACR) (measured together at *m/z* 71) were observed to evolve in the same manner as the primary monoterpene keto-aldehyde(s) and ketone(s), peaking at an approximate mixing ratio of 0.4 (± 0.1) ppbV (Fig. 2e). A series of lower *m/z* ions were also observed to evolve within the reaction chamber, including *m/z* 61 (acetic acid), 59 (acetone), 47 (formic acid), 45 (acetaldehyde), 33 (methanol) and 31 (formaldehyde). Each of these compounds has previously been associated with monoterpene oxidation and/or with off-gassing from illuminated chamber walls. Methanol, acetone and *m/z* 99 (potentially cis-3-hexenal) were also observed within the reaction chamber prior to lights on, with a combined mixing ratio of approximately 20 ppbV.

3.1.2 Particle phase

From inspection of the CPC and SMPS data we see that SOA mass formed during oxidation of the *Betula pendula* air matrix. As can be seen from Fig. 4, during unseeded experiments nucleation occurred immediately after lights on, with no induction period prior to mass formation. After nucleation, SOA mass increased rapidly to ~11 μg m^{-3} by ~40 minutes (experiment 06/07/09), followed by a relatively stable plateau (after the application of wall loss corrections) and a slight increase towards the end of the experiment. In order to suppress nucleation, seed particles were introduced in some experiments, as has been used previously (Dommen et al., 2009;Meyer et al., 2009;Surratt et al., 2007;Kleindienst et al., 2006;Carlton et al., 2009). This more closely represents the conditions encountered in the ambient atmosphere where there is pre-existing aerosol. Consistent with the nucleation experiments described above, SOA mass was observed to increase as soon as the photochemistry was initiated when an ammonium sulphate seed was present (Fig. 4, experiment 07/07/09).

Using the wall-loss-corrected mass data, along with the corresponding quantity of the sum of precursor species reacted and equation (2), SOA yields were obtained for the *Betula pendula* oxidation system:

$$Y_{SOA} = \frac{M_P}{\Delta(\Sigma VOC)} \qquad \text{Eq}^{n}\,(2)$$

In this instance, Y_{SOA} = SOA mass yield, M_P = peak SOA mass (μg m^{-3}) and $\Delta(\Sigma VOC)$ = the sum of gas phase precursors reacted by the time M_p is reached (μg m^{-3}) (Odum et al., 1997). In order to determine $\Delta(\Sigma VOC)$, the time-dependent VOC mixing ratios for total sesquiterpenes, total monoterpenes, camphore and isoprene were independently converted to their corresponding mass concentrations (μg m^{-3}) and the four data sets were combined to give a “total” VOC precursor decay profile. From the total VOC profile, $\Delta(\Sigma VOC)$ was calculated, using the starting mass of ΣVOC at time = 0 and the mass of ΣVOC at the time of M_p. The uncertainty in $\Delta(\Sigma VOC)$ is estimated to be ± 41 %. Using equation (2) for the two *Betula pendula* experiments for which both gas phase mixing ratio and wall-loss-corrected aerosol data were available, SOA yield values of 39 and 26 % were obtained (Fig. 4). It should also be noted that along with previous caveats made regarding the role of the chamber walls and other measurement uncertainties, these yield values also do not take into account the potential loss of particularly "sticky" low volatility compounds (e.g. Ehn et al., 2014) to internal surfaces of the chamber.

It should be noted in the above yield calculations that the partitioning of material between the vapour phase and chamber walls has not been taken into account. Matsunaga and Ziemann (2010) showed that semi-volatile organic compounds move towards equilibrium between the walls and the vapour phase and that the equilibration timescale and equivalent absorptive mass of the walls was dependent on the molecular properties of the partitioning species. Kokkola et al. (2013) demonstrated in their model study that OVOC wall losses will have significant implications on their partitioning between the gas and particle phase, such that the mass components of very low volatility will almost completely be depleted to the chamber walls during the experiment while the depletion of OVOCs of higher volatilities is less efficient. The implications of such partitioning to chamber walls are such that comparison between any yields determined experimentally in different chambers should be conducted with caution. Even when calculated from experiments in the same chamber, yields should be interpreted qualitatively and relatively and not extrapolated to the atmosphere.

3.2 Experiments with tropical species

3.2.1 Gas phase

In order to study the contrast between species that primarily emit monoterpenes and those that primarily emit isoprene, and hence to better understand the isoprene-SOA system, the coupled plant chamber-reaction chamber system was employed to study several tropical species. Two species of fig and one species of palm were selected during the pre-experiment screening process. Those experiments using the figs, *Ficus cyathistipula* and *Ficus benjamina* gave the most complete data set; hence their results are used as a focus for discussion.

Fig. 5 shows the temporal evolution of a number isoprenoids detected in both the plant and reaction chambers (a and b) and the concomitant evolution of a selection of isoprenoid oxidation products (c and d), during a typical *Ficus benjamina* experiment (23/06/09). During a typical *Ficus benjamina* experiment, approximately thirty precursor and product-ion peaks were observed by the CIR-TOF-MS and PTR-MS in the gas phase. Tentative product identification is reported in the supplementary information (Fig. 6, Tables S1 – S5). A similar set of ions was observed during a typical *Ficus cyathistipula* experiment.

From inspection of Fig. 5(a) and (b), the dominance of isoprene in the *Ficus benjamina* system is clear, with 12.3 (± 4.1) ppbV isoprene detected in the reaction chamber at lights on, compared to 0.8 (± 0.4) ppbV monoterpenes, 0.5 (± 0.9) ppbV sesquiterpenes and an estimated 2.7 (± 0.6) ppbV camphore. Speciation of the monoterpenes by GC-MS indicated that the most dominantly emitted C_{10} compounds for *Ficus benjamina* were α-pinene, limonene, sabinene and linalool and for *Ficus cyathistipula* were α-pinene, β-pinene and limonene (Table 2). The sequiterpenes, β-caryophyllene and α-cubebene were also identified.

Products of isoprene were observed to dominate the evolving *Ficus benjamina* and *Ficus cyathistipula* oxidation systems, with the isobaric primary species MACR and MVK comprising the strongest signals (measured together at *m/z* 71). For example, during the *Ficus benjamina* experiment of 23/06/09, a combined peak MACR + MVK mixing ratio of 2.9 (± 0.7) ppbV was observed (Fig. 5c).

Along with MACR and MVK, a series of other ions also associated with isoprene oxidation were detected during *Ficus benjamina* oxidation, including *m/z* 117 and 99 (4-hydroxy-2-methyl-but-2-enoic acid), 103 (C5-alkenediols, C4-hydroxydialdehydes and MPAN), 87 (C4-hydroxycarbonyls and methacrylic acid), 83 (3-methyl furan), 75 (hydroxy acetone) and 31 (formaldehyde). Additionally, a signal of *m/z* 101 was also measured, possibly corresponding to the sum of a series of C5-hydroxycarbonyls and C5-hydroxy hydroperoxides (Tuazon and Atkinson, 1990; Paulson and Seinfeld, 1992; Jenkin *et al.*, 1997; Benkelberg *et al.*, 2000; Sprengnether *et al.*, 2002, Benkelberg *et al.*, 2000; Zhao *et al.*, 2004; Surratt *et al.*, 2006; http://mcm.leeds.ac.uk/MCM, v3.1). Of the signals observed, those of *m/z* 83 and 87 (tentatively assigned to be 3-methyl furan and C4-hydroxycarbonyls/methacrylic acid), were the greatest in magnitude after MACR + MVK (Fig. 6). The temporal evolution of the sum of all of these products suggests that they are predominantly secondary in nature, forming in the chamber after MACR and MVK. They continued to increase in magnitude as the isoprene signal decreased and as the MACR + MVK signal began to fall (Figs. 5 and 6). During a typical *Ficus benjamina* experiment, the sum of these isoprene products was estimated to reach a peak mixing ratio of ~ 1.7 ppbV.

A series of lower molecular weight ions were also observed to evolve within the reaction chamber, including *m/z* 61 (acetic acid), 47 (formic acid), 45 (acetaldehyde), 33 (methanol) and 31 (formaldehyde). Each of these compounds has previously been associated with isoprene oxidation and/or with off-gassing from illuminated chamber walls. The *m/z* 43 and 46 signals, indicative of carbonyls and nitrates, respectively, were also observed to increase significantly during photo-oxidation, indicating the formation and evolution of such species with increasing experiment duration.

Besides ions pertaining to the oxidation products of isoprene, a number of spectral features typically derived from monoterpene oxidation products were also observed to form and evolve in the reaction chamber, including, *m/z* 151, 125, 109, 107, 93 and 91. To a first order approximation, the total peak quantity of oxidation products not believed to result from isoprene decay was estimated to be of the order 2 ppbV. However, it should be noted that the presence of isobaric interference in such a complex system, uncharacterised fragmentation, detection limits and the use of pseudo and averaged calibration sensitivities, impose a certain level of unknown uncertainty upon this final value.

3.2.2 Particle phase

Contrary to the immediate and abundant formation of new particles in the un-seeded *Betula pendula* experiments, the total number of particles and total aerosol mass did not increase above background levels after lights were turned on in the un-seeded tropical *Ficus benjamina* experiments. Figure 7 shows the observed and wall-loss-corrected particle mass concentration during two typical *Ficus benjamina* experiments (22/06/09 and 23/06/09) along with a chamber background experiment. Owing to a lack of particle nucleation in those experiments, the total particle number concentration was too low for the wall loss correction (described in section 2.3) to be implemented. Instead, the average of the wall loss constants determined for the seeded experiments was used to calculate the wall loss corrected mass concentrations reported in Figure 7.

Figure 8 shows the observed and wall-loss-corrected particle mass concentration for ammonium sulphate seeded experiments using VOC emissions of *Ficus benjamina* and *Ficus cyathistipula*, as well as a seeded background experiment. The mass at the start of the experiment represents the initial ammonium sulphate mass. In order to quantify the formation of SOA mass during these experiments, the mass increase relative to the starting seed mass was determined in Figure 9 by subtracting the initial ammonium sulphate seed mass from the total wall loss corrected mass. The same calculation was also performed for the *Betula pendula* seeded experiment (07/07/09). In contrast to the unseeded *Ficus benjamina* and *Ficus Cyathistipula* experiments, SOA mass was observed to form when a seed was present in the reaction chamber. The calculated SOA traces in Figure 9 illustrate a slower build-up of mass during the isoprene dominated *Ficus benjamina* (15/07/09) and *Ficus Cyathistipula* (30/06/09 and 02/07/09) experiments compared to the much faster SOA mass formation in the monoterpene dominated *Betula pendula* experiment. Peak masses of the order 1.3 – 5.5 μg m^{-3} were observed, which when employed with the methodology described in section 3.1.2, produce SOA yields of 10 and 14 % for each of the two *Ficus Cyathistipula* experiments for which both gas and wall-loss-corrected aerosol data were available, i.e. 30/06/09 and 02/07/09, respectively (Fig. 9). Uncertainty in $\Delta(\Sigma VOC)$ is estimated to be ± 47 % and in the size distribution measurements used in the wall loss calculations, of the order of ± 2 %. The uncertainties in the wall-loss correction will likely be substantially greater, but remain unquantified at present.

Discussion and Conclusions

4.1 Betula pendula

In this study we coupled a plant chamber to a photochemical reaction chamber in order to investigate secondary organic aerosol production from a biogenically consistent mixture of biogenic volatile organic compounds. We studied silver birch

(*Betula pendula*), which emits predominantly monoterpenes, with some sesquiterpenes and oxygenated VOCs but only trace isoprene (Table 2, Fig 3).

Our *Betula pendula* experiments showed significant SOA formation (Fig. 4) both in the presence and absence of an ammonium sulphate seed, and reproduced the rate of production and growth of SOA observed in earlier published studies (Mentel et al., 2009;Carlton et al., 2009;e.g. VanReken et al., 2006;Hallquist et al., 2009;Kiendler-Scharr et al., 2009a;Kiendler-Scharr et al., 2009b).

The SOA yield values of 39 and 26 % obtained here for *Betula pendula* compare reasonably well with those reported within the literature for single precursor work conducted under similar conditions. For instance, for the two most abundant monoterpenes emitted by *Betula pendula*, i.e. α-pinene and β-pinene, single precursors yields of the order 1 – 43 (16) and 3 – 30 %, respectively, have been observed (values given in parenthesis were obtained from the Manchester aerosol chamber). Similarly for other common monoterpenes such as limonene, myrcene, Δ3-carene and α-terpenine, SOA yields of 9 – 34, 6 – 43 (15), 2 – 38 and 8 – 25 %, respectively, have been reported and for β-caryophyllene, 37 – 79 (50) % (Lee at al., 2006a and references therein; Alfarra at al., 2012). In a comparable study to ours, Mentel et al., (2009) reported a fractional mass yield of 11 % for their *Betula pendula* experiments, i.e. slightly lower than those given here, but within the bounds of quantified experimental errors. The yield values obtained here for the *Betula pendula* mesocosm system lie roughly in the middle of the single precursor yield range.

As can be seen from inspection of Fig. 3, the transfer of mass through the *Betula pendula* experiment appeared roughly conservative, with a small and steady loss of measured mass from the reaction matrix after ~ 220 min. With the addition of oxygen to the starting body of hydrocarbon material during such an experiment, the total measured mass (i.e. ΣVOCs + SOA) within the system would be expected to increase with time. The absence of such a total measured mass gain (and indeed the mass deficit observed towards the end of the experiment), can most likely be accounted for by considering the various measurement uncertainties involved in producing these data (e.g. assumptions in PTR sensitivity, uncharacterised fragmentation following ionisation, instrument detection limits, etc.) and influences imposed by the chamber walls (including potential loss of more highly oxidised material from the gas phase and greater than expected loss of SOA). Indeed, there is potential for a system mass increase by the end of the experiment to lie within the uncertainty bounds of the CIR-TOF-MS/PTR-MS measurements alone, e.g. the average, single compound PTR measurement uncertainty is ~ ± 30 %, allowing the final measured value of 130 μg m^{-3} to have an upper limit of 170 μg m^{-3}, i.e. greater than the starting value. Considering these results it seems that the system studied is reasonably well characterised given the complications involved in such a task.

Certain insights into the mechanisms of SOA formation and growth during the *Betula pendula* experiments can be obtained through a combined examination of the VOC data, the time-dependent growth curves (Fig. 10) and the aerosol composition data. The data in Fig. 10 demonstrates that during oxidation of the *Betula pendula* emissions and in absence of a seed, SOA mass evolution can be roughly split into two phases. In the early stages of the experiment after nucleation, SOA mass growth increased somewhat rapidly with respect to the amount of precursors reacted; however, after roughly 30 % of the initial precursor mass had been consumed, the rate of mass growth with respect to VOC precursor consumption was observed to reach an approximate steady state. When ammonium sulphate seed was present within the chamber, there was a similarly rapid initial growth with respect to VOC consumption, however this time subsequent aerosol evolution was characterised by a roughly linear mass increase to a much higher final mass by the end of the experiment. Considering the various species of precursor VOCs detected in the *Betula pendula* plant chamber air, and the relative lifetimes of these VOCs, it would seem possible that initially the shorter-lived sesquiterpenes react to form a significant proportion of the high mass, nucleating/condensing species, before being removed from the system (e.g. Jenkin et al., 2012). Subsequent aerosol mass formation as the air in the reaction chamber ages towards the central phase of the experiment, is then likely to result from the partitioning of relatively more volatile products formed from slower reacting monoterpenes, e.g. products such as pinic and pinonic acid from α-pinene oxidation (e.g. Jenkin, 2004; Camredon et al., 2010), and products such as the primary acyclic unsaturated aldehydes, (*m/z* 111 + 93); the temporal profile of which demonstrates gas-phase loss concomitant with wall-loss-corrected aerosol growth reaching a steady state.

Further understanding of the composition and evolution of SOA typical of temperate plant environs comes from investigation of Figure 11, which shows the evolution of the fraction of the ratio of more/less oxygenated material present in the aerosol during the initial stages of a typical unseeded *Betula pendula* experiment (06/07/09). Figure 11 was constructed using the ratio of *m/z* 44 to 43 obtained from the AMS (*i.e. f*44/43, where *m/z* 44 is derived from "more" oxidised material and *m/z* 43 from "less" oxidised material, Ng et al., 2010). In this instance, the *f*44/43 ratio exhibits linear growth with time, from a value of ~ 0.8 to ~ 1.1, suggesting an increase in the oxygenated content of the aerosol as the experiment ages. Such an increase in oxygenated content is generally observed when precursor species contain multiple C=C bonds (e.g. ocimene and myrcene), offering significant potential for higher aerosol O:C composition (e.g. perhaps species such as acyclic unsaturated aldehydes and their subsequent generations of products). Indeed, the evolution of the *f*44/43 ratio observed here is consistent with those results obtained from single precursor experiments investigating the acyclic monoterpene, myrcene and the sesquiterpene, β-caryophyllene (Alfarra et al., 2012; Alfarra et al., 2013).

Off-line compositional analysis of the SOA collected at the end of the *Betula pendula* experiments supports the findings obtained from the on-line gas phase and bulk aerosol composition data. The LC-MS^2 analysis produced chromatograms with peaks matching those seen in comparable single precursor BVOC experiments, with tracer compounds of both sesquiterpene and monoterpene SOA, detected (Fig. 12). Amongst the compounds observed were those of molecular weight (MW) 238, 242, 254 and 256, corresponding to 4-(3,3-dimethyl-2-(3-oxopropyl)cyclobutyl)pent-4-enoic acid, 3-(3,3-dimethyl-2-(3-oxobutyl)cyclobutyl)-3-hydroxypropanoic acid, β-nocaryophyllonic acid/β-caryophyllinic acid and β-nocaryophyllinic acid, respectively, produced during β-caryophyllene oxidation (e.g. Alfarra et al., 2013) and MW 184, corresponding to cis-pinonic acid, produced during α-pinene oxidation. Many other terpene oxidation tracers were detected, including compounds of molecular weight 118 and 200, which are also prevalent in SOA obtained from single precursor myrcene experiments. This observation is in line with findings obtained from the gas phase data, which suggest a relatively significant presence of gaseous acyclic unsaturated aldehydes that would originate from acyclic unsaturated terpenes, such as myrcene.

4.2 Tropical species

In addition to *Betula pendula*, we studied three tropical plant species: two figs (*Ficus benjamina* and *Ficus cyathistipula*) and one palm (*Caryota millis*); in this work, we focus on results obtained from the fig plants. All three tropical species were found to be strong isoprene emitters, with very much smaller emissions of monoterpenes, sesquiterpenes, and oxygenated VOCs (Table 2, Fig. 6).

During the tropical plant experiments, the primary gas-phase isoprene oxidation products MACR, MVK, formaldehyde, isoprene hydroxy hydroperoxides and the secondary product hydroxyacetone were all observed (e.g. Figs. 5 and 6 and Tables S4 and S5 in the supplementary information). MACR, the isoprene hydroxy hydroperoxides (isoprene epoxide (IEPOX) and isoprene hydroperoxide (ISOPOOH)) and hydroxyacetone are all believed to be precursors to SOA formation (Jaoui et al., 2010;Carlton et al., 2009;Kleindienst et al., 2009;Paulot et al., 2009;Kleindienst et al., 2007;Lee et al., 2006;Kroll et al., 2006;Surratt et al., 2006;Claeys et al., 2004b;Rollins et al., 2009;Robinson et al., 2010). In this study, with the exception of MACR and MVK, these products all formed at yields lower than those previously reported (Table 3), with MACR + MVK, hydroperoxides, hydroxy acetone and formaldehyde being observed to form in yields of 17 – 36, 1 – 3, 0 – 2 and 2 – 7 %, respectively during our work. This disagreement may result from differences in OH concentrations and NO_x concentrations in each of the experimental studies. Other isoprene products tentatively identified from the CIR-TOF-MS and PTR-MS data include, C5-alkenediols, C4-hydroxycarbonyls/methacrylic acid and 3-methyl furan (Table S4), which have also previously been associated with SOA formation (e.g. Claeys et al., 2004; Surratt et al., 2006; Robinson et al., 2010). For a typical *Ficus benjamina* experiment (23/06/09) the sum of these and other potential isoprene products, excluding MACR + MVK, was estimated to have a combined gas phase yield of the order 18 % (Fig. 5).

As can be seen in Fig. 6 mass transfer through the *Ficus benjamina* system was characterised by a slight mass decrease just after the start of the experiment followed by a gradual increase in mass with time. As was stated in section 4.1 a mass increase is expected with time during such an experiment, owing to the addition of oxygen to the precursor hydrocarbon material. Consequently, when considering the data presented in Fig. 6 in the context of potential uncertainties involved (including difficult to characterise influences imposed by the chamber walls), it appears that the system being studied is reasonably well characterised.

By comparing Figs. 3 and 6 we see that the monoterpene dominated *Betula pendula* system, which produces larger and lower vapour pressure oxidation products than the isoprene dominated *Ficus* system, as well as measureable SOA, is the case which exhibits measured mass loss. From this contrast it is reasonable to assume a significant fraction of any mass deficit observed during *Betula pendula* oxidation could result from the loss of the heavier, lower volatility compounds that are present in the *Betula pendula* oxidation system but not in the *Ficus* system.

Despite the detection of a number of first- and second-generation gas phase products that have previously been directly linked with isoprene SOA composition (Claeys et al., 2004; Wang et al., 2004; Edney et al., 2005; Surratt et al., 2006; Healy et al., 2008), there was no accompanying evidence of SOA formation from the isoprene-emitting tropical plants during unseeded, nucleation style experiments (Fig. 7). A lack of SOA mass formation during our unseeded *Ficus benjamina* experiments could have resulted from a number of different factors, not least of which was simply the absence of a seed surface (acidic or otherwise) to help facilitate partitioning of the semi-volatile oxidation products to the aerosol phase and produce particles of sufficient size and measureable particle mass (e.g. Kroll et al., 2006). Another potentially significant contributing factor in suppressing SOA formation during these experiments was our relatively low VOC/NO_x ratio and the resultant gas phase chemistry. In the presence of high (i.e. ppbV-level) NO_x mixing ratios, RO_2 radicals react with NO to produce mainly alkoxy (RO) radicals. For low molecular mass VOCs such as isoprene, these RO radicals generally fragment into smaller, more volatile products that do not easily partition from the gas phase to the aerosol phase, resulting in a low SOA yield (Surratt *et al.,* 2010). Conversely, under low NO_x conditions, RO_2 radicals are known to undergo self- and cross-reactions to produce organic peroxides and hydroperoxides of relatively low volatility. For example, Surratt *et al.* (2010) showed that under high NO_x conditions the yield of the potentially SOA forming gas phase IEPOX was reduced with respect to the equivalent value under low NO_x conditions, where IEPOX formed in substantial yields (upward of 75 %) from the further oxidation of ISOPOOH by OH.

In contrast to our unseeded *Ficus* experiments, when an ammonium sulphate seed was present (and following wall loss correction), SOA mass was observed to form and evolve within the reaction chamber (Fig. 9). From estimates of the total concentrations of precursor VOCs within the reaction chamber matrix (primarily isoprene, e.g. Fig. 5), an SOA mass yield of the order 10 – 14 % was obtained for the *Ficus Cyathistpula* system. If it were to be assumed that the SOA were solely formed from oxidation products of isoprene as the major emitted VOC, this yield would appear excessive in comparison with those obtained previously from single precursor isoprene studies, i.e. ~ 0.1 – 5.5 % (van Donkelaar et al., 2007;Kleindienst et al., 2009, 2007;Kroll et al., 2005, 2006;Claeys et al., 2004a;Edney et al., 2005(van Donkelaar et al., 2007;Kleindienst et al., 2009, 2007;Kroll et al., 2005, 2006;Claeys et al., 2004a;Edney et al., 2005; Brégonzio-Rozier et al., 2014). However, we must consider that the mesocosm system is in fact an ensemble of precursors, albeit an ensemble dominated by isoprene, analogous to ambient air above a tropical forested region (Hewitt et al., 2010; MacKenzie et al., 2011).

For the experiments of 30/06/09 and 02/07/09, for which SOA yields were obtained for the *Ficus Cyathistpula* system, a fraction of camphore was also observed in the air entering the reaction chamber (presumably for these two particular experiments, sesquiterpenes and monoterpenes were present at concentrations below the detection limits of the PTR-MS and CIR-TOF-MS). The concentration of camphore at lights on was estimated to be ~ 0.5 – 0.9 ppbV for the *Ficus cyathistipula* system and ~ 1.4 – 2.7 ppbV for *Ficus benjamina,* and the sum of all *non-precursor* ions in the CIR-TOF-MS mass spectrum > *m/z* 100 (indicative of *non-isoprene-like* oxidation products; excluding *m/z* 103 and 117) was estimated to be of the order 2 ppbV by the end of the experiments. This calculation approximates the *m/z* > 100 summation as one large, multifunctional analyte with a PTR sensitivity similar to pinonaldehyde (a typical, multifunctional, high MW molecule resulting from terpene oxidation). Continuing this assumption and taking a range of known VOC terpene product yields

(Y^{P}_{VOC}) obtained from previous work at the Manchester chamber (i.e. Y^{P}_{VOC} = 100 % the limiting case; 77 % from *Ficus Benjamina* oxidation; 55 % from *Betula Pendula* oxidation; and 29 % for pinonaldehyde and $\Sigma(I_{111}, I_{93})$), a *non-isoprene* $VOC_{precursor}$ concentration may be estimated. Taking a range of known SOA yields obtained from the same reaction chamber (i.e. α-pinene, myrcene, linalool and β-caryophyllene; Alfarra et al., 2013), the SOA yield obtained here for the *Betula pendula* system and the estimate of [$VOC_{precursor}$], Eqn. (2) may be solved to provide a crude estimate of the mass of SOA formed from *non-isoprene* precursors. Consequently, an estimate of the residual SOA mass derived from isoprene oxidation within the *Ficus* system can be inferred for each of the experiments shown in Fig. 9.

For 78 of the 120 measurement-and-parameter sets tested, the estimated residual SOA mass resulting solely from isoprene oxidation was negative – i.e., production of SOA from isoprene oxidation was not required to close the mass balance. Values were calculated based on the widest range of peak masses observed during the *ficus* experiments (M_p = 1.3 µg m^{-3} and 5.5 µg m^{-3}), and assume the lowest (29 %) and highest (100 %) VOC terpene yields and lowest (5 %) and highest (47 %) SOA yields from non-isoprene precursors, respectively, as observed in previous experiments conducted within this chamber. These ranges result in calculated residual SOA mass of -28.5 to +5.0 µg m^{-3} produced solely from isoprene oxidation. Hence, there are combinations of measurements, observations and oxidation/phase-change parameters — omitting isoprene and its oxidation products — that can account for ~20 times the observed aerosol mass production, and other combinations of measurements and parameters that leave up to ~ 90 % of the condensed mass to be explained by isoprene oxidation. If, instead of using the limiting cases, the closest approximation to the *ficus cyathistipula* system is used (i.e. Y_{VOC} = 77 % and Y_{SOA} = Y_{SOA} = *a*-pinene = 15 %), non-isoprene products could have accounted for around 145 % of the SOA mass that was produced. We have no way of assigning formal likelihoods to each set of measurements and parameters in this exercise, but we note that the great preponderance of parameter combinations do not require an isoprene contribution to the SOA mass (i.e. 78/120 measurement-and-parameter sets tested) under our experimental conditions. Moreover, our experiments produce much less SOA mass than would be expected from published experiments using individual mono- and sesquiterpenes.

There are three principal reasons why the estimates of aerosol production from isoprene in the tropical plant experiments span such a large range. Firstly, the plants in the mesocosm emit a complicated mixture of biogenic VOCs, some of which are known to oxidise much more rapidly than isoprene and which will produce condensable compounds when oxidised. Secondly, these minor compounds co-emitted from principally-isoprene emitting tropical trees are imperfectly quantified because of the sensitivity of the chemical ionisation (PTR and CIR) instruments. Thirdly, these minor co-emissions are imperfectly characterised because many higher molecular weight compounds, such as the mono- and sesquiterpenes, are isobaric in the PTR and CIR instruments and so precise chemical structures cannot easily be assigned. Without better instrument detection sensitivity and high time resolution chemical identification for the reactive compounds co-emitted with isoprene, it is not possible to constrain further the aerosol yield from the tropical plants. Unfortunately, insufficient SOA mass formed during *Ficus* experiments to allow us to conduct any form of compositional analysis.

4.3 Atmospheric significance

Our results are specific to VOC/NO_x ratios of 3 - 9 and NO_x mixing ratios of ~ 2 ppbV. Note, however, that the three reasons given above for the uncertainty in the aerosol production ascribed to isoprene in our experiments will also pertain to field measurements, often being exacerbated by variability and the difficulties of operating in the field. A contribution of isoprene to SOA is *supported* by recent observations of isoprene related SOA formation above the tropical forest of Danum Valley, Borneo, a high isoprene, low NO_x region (typical ratio of 20:1, isoprene/NO_x) (Hewitt et al., 2010b). Robinson *et al* (2010) observed that up to 15 % by mass of atmospheric sub-micron organic aerosol above the tropical forest of Danum Valley was comprised of methyl furan, the most likely source of which is the oxidation of isoprene (i.e. thermal decomposition of isoprene derived SOA) (Ruppert and Becker, 2000;Robinson et al., 2010; Lin et al., 2012; Budisulistiorini et al., 2013). Although much smaller in magnitude, the monoterpene emissions measured at Danum Valley were more than adequate to account for the remaining sub-micron organic aerosol (MacKenzie et al., 2011), just as in the majority of aerosol mass calculations for principally-isoprene-emitting tropical trees, described above.

It has recently been proposed that isoprene can inhibit aerosol formation when present in air containing other potential SOA precursors, such as mono- and sesquiterpenes (Kiendler-Scharr et al., 2009a). Kiendler-Scharr et al. propose that isoprene could effectively act as an OH scavenger, suppressing new particle formation by slowing the oxidation of available monoterpenes (and presumably sesquiterpenes). In line with this thesis, interpretation of the results obtained from our seeded experiments with *Ficus* species leaves room for a potential role for isoprene in inhibiting SOA formation under certain atmospheric conditions, i.e. our results imply that isoprene may impact negatively on the overall SOA forming potential of air containing other biogenic SOA precursors. However, owing to the constraints laid upon our experiments by the instrumentation and apparatus employed, it is difficult to assign a given certainty level to the role played by isoprene in the ambient atmosphere and caution should be taken when interpreting such findings.

The fact that isoprene accounts for approximately 50 % of the total global burden of non-methane VOC, (Guenther et al., 2006), would make it a significant contributor to global SOA. It has been estimated that, even if the secondary organic aerosol yield from isoprene is small (e.g. 1 %), the overall contribution to total atmospheric aerosol could be up to 6 Tg yr^{-1} (Carlton et al., 2009). Van Donkelaar *et al.* (2007) found that using an isoprene SOA yield of 2 % improved the relationship between model simulations and organic aerosol measurements, and contributed 10 – 50 % of the total organic aerosol loading over the United States during the summer. Understanding the exact role played by isoprene in air containing many different VOCs, and being able to account for the differing isoprene SOA yields under contrasting NO_x and acidity (Lin *et al.*, 2012; Lin *et al.*, 2013; Pye *et al.*, 2013) environments, will undoubtedly help to significantly improve global modelling estimates of total SOA loading even further (Couvidat and Seigneur, 2010).

Further to any such potential impacts imposed by isoprene, it has recently been shown that a range of other BVOC emissions, released in response to a range of environmental stress factors, can also have significant impacts on biogenic SOA formation and yield (Mentel et al., 2013). It has been shown that the emissions of sesquiterpenes, methyl salicylate and C_{17} BVOCs, released as a result of certain environmental stress factors have a net positive impact on SOA yield; whereas certain stress induced green leaf volatiles ((Z)-3-hexenol and (Z)-3-hexenylacetate) behave similarly to isoprene, suppressing SOA formation (Mentel et al., 2013).

Given the highly differing reported yields of isoprene SOA under various oxidant schemes, the uncertainty in the exact role played by isoprene and its oxidation products in realistic mixtures of VOCs (in particular in the context of SOA nucleation rates; Kiendler-Scharr et al., 2009) and the lack of knowledge regarding stress induced BVOCs, their atmospheric oxidation and their roles in biogenic SOA formation (and impact on chemical and physical properties), we suggest that there is a pressing requirement for additional, atmosphere-relevant laboratory and field studies to give us the necessary insight to successfully control biogenic SOA (Carlton et al., 2010).

Acknowledgements

The authors gratefully acknowledge the UK Natural Environment Research Council (NERC) for funding of the APPRAISE ACES (NE/E011217/1), ACIDPRUF (NE/I020121/1) and CLAIRE-UK (NE/I012567/1) consortia. The authors would also like to acknowledge support from the EU-FP7 EUROCHAMP-2 project. M. R. Alfarra was supported by UK National Centre for Atmospheric Sciences (NCAS) funding. The authors would like to thank Dr Iain White for his assistance with VOC measurements and instrument calibration. This is paper number 1 from the Birmingham Institute of Forest Research.

5 References

Alfarra, M. R., N. Good, K. P. Wyche, J. E. Hamilton, P. S. Monks, A. C. Lewis and G. McFiggans (2013). "Water uptake is independent of the inferred composition of secondary aerosols derived from multiple biogenic VOCs." Atmospheric Chemistry and Physics **13**(23): 11769-11789. DOI: 10.5194/acp-13-11769-2013.

Alfarra, M. R., J. F. Hamilton, K. P. Wyche, N. Good, M. W. Ward, T. Carr, M. H. Barley, P. S. Monks, M. E. Jenkin, A. C. Lewis and G. B. McFiggans (2012). "The effect of photochemical ageing and initial precursor concentration on the composition and hygroscopic properties of beta-caryophyllene secondary organic aerosol." Atmospheric Chemistry and Physics **12**(14): 6417-6436. DOI: 10.5194/acp-12-6417-2012.

Alfarra, M. R., D. Paulsen, M. Gysel, A. A. Garforth, J. Dommen, A. S. H. Prevot, D. R. Worsnop, U. Baltensperger and H. Coe (2006). "A mass spectrometric study of secondary organic aerosols formed from the photooxidation of anthropogenic and biogenic precursors in a reaction chamber." Atmospheric Chemistry and Physics **6**: 5279-5293.

Alfarra, M. R., D. Paulsen, M. Gysel, A. A. Garforth, J. Dommen, A. S. H. Prévôt, D. R. Worsnop, U. Baltensperger and H. Coe (2006). "A mass spectrometric study of secondary organic aerosols formed from the photooxidation of anthropogenic and biogenic precursors in a reaction chamber." Atmospheric Chemistry and Physics **6**: 5279–5293.

Atkinson, R. and J. Arey (2003). "Gas-phase tropospheric chemistry of biogenic volatile organic compounds: a review." Atmospheric Environment **37**: S197-S219. DOI: 10.1016/s1352-2310(03)00391-1.

Bahreini, R., M. D. Keywood, N. L. Ng, V. Varutbangkul, S. Gao, R. C. Flagan, J. H. Seinfeld, D. R. Worsnop and J. L. Jimenez (2005). "Measurements of secondary organic aerosol from oxidation of cycloalkenes, terpenes, and m-xylene using an Aerodyne aerosol mass spectrometer." Environmental Science and Technology, **39**: 15, 5674-5688

Baltensperger, U., J. Dommen, R. Alfarra, J. Duplissy, K. Gaeggeler, A. Metzger, M. C. Facchini, S. Decesari, E. Finessi, C. Reinnig, M. Schott, J. Warnke, T. Hoffmann, B. Klatzer, H. Puxbaum, M. Geiser, M. Savi, D. Lang, M. Kalberer and T. Geiser (2008). "Combined determination of the chemical composition and of health effects of secondary organic aerosols: The POLYSOA project." Journal of Aerosol Medicine and Pulmonary Drug Delivery **21**(1): 145-154. DOI: 10.1089/jamp.2007.0655.

Benkelberg, H. J., O. Boge, R. Seuwen and P. Warneck (2000). "Product distributions from the OH radical-induced oxidation of but-1-ene, methyl-substituted but-1-enes and isoprene in NOx-free air." Physical Chemistry Chemical Physics **2**(18): 4029-4039. DOI: 10.1039/b002053m.

Blake, R. S., P. S. Monks and A. M. Ellis (2009). "Proton-Transfer Reaction Mass Spectrometry." Chemical Reviews **109**(3): 861-896. DOI: 10.1021/cr800364q.

Blake, R. S., C. Whyte, C. O. Hughes, A. M. Ellis and P. S. Monks (2004). "Demonstration of proton-transfer reaction time-of-flight mass spectrometry for real-time analysis of trace volatile organic compounds." Analytical Chemistry **76**(13): 3841-3845. DOI: 10.1021/ac0498260.

Budisulistiorini, S. H., Canagaratna, M. R., Croteau, P. L., Marth, W. J., Baumann, K., Edgerton, E. S., Shaw, S. L., Knipping, E. M., Worsnop, D. R., Jayne, J. T., Gold, A. and Surratt J. D.: Real-Time Continuous Characterization of Secondary Organic Aerosol Derived from Isoprene Epoxydiols in Downtown Atlanta, Georgia, Using the Aerodyne Aerosol Chemical Speciation Monitor, Environ. Sci. Technol., 47 (11), 686–5694, doi: 10.1021/es400023n, 2013

Brégonzio-Rozier, L., Siekmann, F., Giorio, C., Pangui, E., Morales, S., B., Temime-Roussel, B., Gratien, A., Michoud, V., Ravier, S., Tapparo, A., Monod, A. and Doussin J.-F.: Gaseous products and Secondary Organic Aerosol formation during long term oxidation of isoprene and methacrolein, Atmos. Chem. Phys. Discuss., 14, 22507-22545, 2014

Camredon, M., J. F. Hamilton, M. S. Alam, K. P. Wyche, T. Carr, I. R. White, P. S. Monks, A. R. Rickard and W. J. Bloss (2010). "Distribution of gaseous and particulate organic composition during dark alpha-pinene ozonolysis." Atmospheric Chemistry and Physics **10**(6): 2893-2917.

Canagaratna, M. R., J. T. Jayne, J. L. Jimenez, J. D. Allan, M. R. Alfarra, Q. Zhang, T. B. Onasch, F. Drewnick, H. Coe, A. Middlebrook, A. Delia, L. R. Williams, A. M. Trimborn, M. J. Northway, P. F. DeCarlo, C. E. Kolb, P. Davidovits and D. R. Worsnop (2007). "Chemical and microphysical characterization of ambient aerosols with the aerodyne aerosol mass spectrometer." Mass Spectrometry Reviews **26**(2): 185-222. DOI: :10.1002/mas.20115.

Carlton, A. G., R. W. Pinder, P. V. Bhave and G. A. Pouliot (2010). "To What Extent Can Biogenic SOA be Controlled?" Environmental Science & Technology **44**(9): 3376-3380.

Carlton, A. G., C. Wiedinmyer and J. H. Kroll (2009). "A review of Secondary Organic Aerosol (SOA) formation from isoprene." Atmospheric Chemistry and Physics **9**(14): 4987-5005.

Carslaw, K. S., O. Boucher, D. V. Spracklen, G. W. Mann, J. G. L. Rae, S. Woodward and M. Kulmala (2010). "A review of natural aerosol interactions and feedbacks within the Earth system." Atmos. Chem. Phys. **10**(4): 1701-1737.

Carvalho, L. R. F., P. C. Vasconcellos, W. Mantovani, C. S. Pool and S. O. Pisani (2005). "Measurements of biogenic hydrocarbons and carbonyl compounds emitted by trees from temperate warm Atlantic rainforest, Brazil." Journal of Environmental Monitoring **7**(5): 493-499. DOI: 10.1039/b414881a.

Claeys, M., B. Graham, G. Vas, W. Wang, R. Vermeylen, V. Pashynska, J. Cafmeyer, P. Guyon, M. O. Andreae, P. Artaxo and W. Maenhaut (2004). "Formation of secondary organic aerosols through photooxidation of isoprene." Science **303**(5661): 1173-1176.

Claeys, M., W. Wang, A. C. Ion, I. Kourtchev, A. Gelencser and W. Maenhaut (2004). "Formation of secondary organic aerosols from isoprene and its gas-phase oxidation products through reaction with hydrogen peroxide." Atmospheric Environment **38**(25): 4093-4098. DOI: 10.1016/j.atmosenv.2004.06.001.

Couvidat, F. and C. Seigneur (2010). "Modeling secondary organic aerosol formation from isoprene oxidation under dry and humid conditions." Atmos. Chem. Phys. Discuss. **10**(8): 20559-20605.

Dommen, J., H. HelleÌn, M. Saurer, M. Jaeggi, R. Siegwolf, A. Metzger, J. Duplissy, M. Fierz and U. Baltensperger (2009). "Determination of the Aerosol Yield of Isoprene in the Presence of an Organic Seed with Carbon Isotope Analysis." Environmental Science & Technology **43**(17): 6697-6702.

Donahue, N. M., A. L. Robinson and S. N. Pandis (2009). "Atmospheric organic particulate matter: From smoke to secondary organic aerosol." Atmospheric Environment **43**(1): 94-106.

Drewnick, F., S. S. Hings, P. DeCarlo, J. T. Jayne, M. Gonin, K. Fuhrer, S. Weimer, J. L. Jimenez, K. L. Demerjian, S. Borrmann and D. R. Worsnop (2005). "A new time-of-flight aerosol mass spectrometer (TOF-AMS) - Instrument description and first field deployment." Aerosol Science and Technology **39**(7): 637-658. DOI: 10.1080/02786820500182040.

Ehn, M., Thornton, J. A., Kleist, E., Sipila, M., Junninen, H., Pullinen, I., Springer, M., Rubach, F., Tillmann, R., Lee, B., Lopez-Hilfiker, F., Andres, S., Acir, I. H., Rissanen, M., Jokinen, T., Schobesberger, S., Kangasluoma, J., Kontkanen, J., Nieminen, T., Kurten, T., Nielsen, L. B., Jorgensen, S., Kjaergaard, H. G., Canagaratna, M., Dal Maso, M., Berndt, T., Petaja, T.,Wahner, A., Kerminen, V. M., Kulmala, M., Worsnop, D. R., Wildt, J., and Mentel, T. F.: A large source of low-volatility secondary organic aerosol, Nature, 506 (7489), 476-479, doi: 10.1038/nature13032, 2014

Edney, E. O., T. E. Kleindienst, M. Jaoui, M. Lewandowski, J. H. Offenberg, W. Wang and M. Claeys (2005). "Formation of 2-methyl tetrols and 2-methylglyceric acid in secondary organic aerosol from laboratory irradiated isoprene/NOX/SO2/air mixtures and their detection in ambient PM2.5 samples collected in the eastern United States." Atmospheric Environment **39**(29): 5281-5289. DOI: 10.1016/j.atmosenv.2005.05.031.

Geron, C., S. Owen, A. Guenther, J. Greenberg, R. Rasmussen, J. Hui Bai, Q.-J. Li and B. Baker (2006). "Volatile organic compounds from vegetation in southern Yunnan Province, China: Emission rates and some potential regional implications." Atmospheric Environment **40**(10): 1759-1773.

Guenther, A., T. Karl, P. Harley, C. Wiedinmyer, P. I. Palmer and C. Geron (2006). "Estimates of global terrestrial isoprene emissions using MEGAN (Model of Emissions of Gases and Aerosols from Nature)." Atmospheric Chemistry and Physics **6**: 3181-3210.

Guenther, A. B., X. Jiang, C. L. Heald, T. Sakulyanontvittaya, T. Duhl, L. K. Emmons and X. Wang (2012). "The Model of Emissions of Gases and Aerosols from Nature version 2.1 (MEGAN2.1): an extended and updated framework for modeling biogenic emissions." Geosci. Model Dev. **5**(6): 1471-1492. DOI: 10.5194/gmd-5-1471-2012.

Gunthe, S. S., S. M. King, D. Rose, Q. Chen, P. Roldin, D. K. Farmer, J. L. Jimenez, P. Artaxo, M. O. Andreae, S. T. Martin and U. Poschl (2009). "Cloud condensation nuclei in pristine tropical rainforest air of Amazonia: size-resolved measurements and modeling of atmospheric aerosol composition and CCN activity." Atmospheric Chemistry and Physics **9**(19): 7551-7575.

Hallquist, M., J. C. Wenger, U. Baltensperger, Y. Rudich, D. Simpson, M. Claeys, J. Dommen, N. M. Donahue, C. George, A. H. Goldstein, J. F. Hamilton, H. Herrmann, T. Hoffmann, Y. Iinuma, M. Jang, M. E. Jenkin, J. L. Jimenez, A. Kiendler-Scharr, W. Maenhaut, G. McFiggans, T. F. Mentel, A. Monod, A. S. H. Prevot, J. H. Seinfeld, J. D. Surratt, R. Szmigielski and J. Wildt (2009). "The formation, properties and impact of secondary organic aerosol: current and emerging issues." Atmospheric Chemistry and Physics **9**(14): 5155-5236.

Hamilton, J. F., Alfarra, M. R., Robinson, N., Ward, M. W., Lewis, A. C., McFiggans, G. B., Coe, H., and Allan, J. D.: Linking biogenic hydrocarbons to biogenic aerosol in the Borneo rainforest. Atmos. Chem. Phys., 13(22), 11295-11305, doi:10.5194/acp-13-11295-2013, 2013.

Healy, R. M., J. C. Wenger, A. Metzger, J. Duplissy, M. Kalberer and J. Dommen (2008). "Gas/particle partitioning of carbonyls in the photooxidation of isoprene and 1,3,5-trimethylbenzene." Atmospheric Chemistry and Physics **8**(12): 3215-3230.

Hewitt, C. N., J. D. Lee, A. R. MacKenzie, M. P. Barkley, N. Carslaw, G. D. Carver, N. A. Chappell, H. Coe, C. Collier, R. Commane, F. Davies, B. Davison, P. Di Carlo, C. F. Di Marco, J. R. Dorsey, P. M. Edwards, M. J. Evans, D. Fowler, K. L. Furneaux, M. Gallagher, A. Guenther, D. E. Heard, C. Helfter, J. Hopkins, T. Ingham, M. Irwin, C. Jones, A. Karunaharan, B. Langford, A. C. Lewis, S. F. Lim, S. M. MacDonald, A. S. Mahajan, S. Malpass, G. McFiggans, G. Mills, P. Misztal, S. Moller, P. S. Monks, E. Nemitz, V. Nicolas-Perea, H. Oetjen, D. E. Oram, P. I. Palmer, G. J. Phillips, R. Pike, J. M. C. Plane, T. Pugh, J. A. Pyle, C. E. Reeves, N. H. Robinson, D. Stewart, D. Stone, L. K. Whalley and X. Yin (2010). "Overview:

oxidant and particle photochemical processes above a south-east Asian tropical rainforest (the OP3 project): introduction, rationale, location characteristics and tools." Atmospheric Chemistry and Physics **10**(1): 169-199.

Hewitt, C. N., J. D. Lee, A. R. MacKenzie, M. P. Barkley, N. Carslaw, G. D. Carver, N. A. Chappell, H. Coe, C. Collier, R. Commane, F. Davies, B. Davison, P. DiCarlo, C. F. Di Marco, J. R. Dorsey, P. M. Edwards, M. J. Evans, D. Fowler, K. L. Furneaux, M. Gallagher, A. Guenther, D. E. Heard, C. Helfter, J. Hopkins, T. Ingham, M. Irwin, C. Jones, A. Karunaharan, B. Langford, A. C. Lewis, S. F. Lim, S. M. MacDonald, A. S. Mahajan, S. Malpass, G. McFiggans, G. Mills, P. Misztal, S. Moller, P. S. Monks, E. Nemitz, V. Nicolas-Perea, H. Oetjen, D. E. Oram, P. I. Palmer, G. J. Phillips, R. Pike, J. M. C. Plane, T. Pugh, J. A. Pyle, C. E. Reeves, N. H. Robinson, D. Stewart, D. Stone, L. K. Whalley and X. Yin (2010). "Overview: oxidant and particle photochemical processes above a south-east Asian tropical rainforest (the OP3 project): introduction, rationale, location characteristics and tools." Atmos. Chem. Phys. **10**(1): 169-199.

Holzinger, R., A. Lee, K. T. Paw and A. H. Goldstein (2005). "Observations of oxidation products above a forest imply biogenic emissions of very reactive compounds." Atmospheric Chemistry and Physics **5**: 67-75.

Pye, H. O. T., Pinder, R. W., Piletic, I. R., Xie, Y., Capps, S. L., Lin, Y. H., Surratt, J. D., Zhang, Z., Gold, A., Luecken, D. J., Hutzell, W. T., Jaoui, J., Offenberg, J. H., Kleindienst, T. E., Lewandowski, M., and Edney E. O.: Epoxide Pathways Improve Model Predictions of Isoprene Markers and Reveal Key Role of Acidity in Aerosol Formation, Environ. Sci. Technol., 47 (19), 11056–11064, doi: 10.1021/es402106h, 2013

IPCC (2007). Climate change 2007: The Physical Science Basis, Cambridge University Press, Cambridge.

Isaksen, I. S. A., C. Granier, G. Myhre, T. K. Berntsen, S. B. Dalsoren, M. Gauss, Z. Klimont, R. Benestad, P. Bousquet, W. Collins, T. Cox, V. Eyring, D. Fowler, S. Fuzzi, P. Jockel, P. Laj, U. Lohmann, M. Maione, P. Monks, A. S. H. Prevot, F. Raes, A. Richter, B. Rognerud, M. Schulz, D. Shindell, D. S. Stevenson, T. Storelvmo, W. C. Wang, M. van Weele, M. Wild and D. Wuebbles (2009). "Atmospheric composition change: Climate-Chemistry interactions." Atmospheric Environment **43**(33): 5138-5192. DOI: 10.1016/j.atmosenv.2009.08.003.

Jang, M. S., N. M. Czoschke, S. Lee and R. M. Kamens (2002). "Heterogeneous atmospheric aerosol production by acid-catalyzed particle-phase reactions." Science, 298, 814-817.

Jaoui, M., E. W. Corse, M. Lewandowski, J. H. Offenberg, T. E. Kleindienst and E. O. Edney (2010). "Formation of organic tracers for isoprene SOA under acidic conditions." Atmospheric Environment **In Press, Corrected Proof**.

Jenkin, M. E., S. M. Saunders, and M. J. Pilling (1997). "The tropospheric degradation of volatile organic compounds: a protocol for mechanism development." Atmospheric Environment **31**(1): 81-104, 1997.

Jenkin, M. E. (2004). "Modelling the formation and composition of secondary organic aerosol from alpha- and beta-pinene ozonolysis using MCM v3." Atmospheric Chemistry and Physics **4**: 1741-1757.

Jenkin, M. E., K. P. Wyche, C. J. Evans, T. Carr, P. S. Monks, M. R. Alfarra, M. H. Barley, G. B. McFiggans, J. C. Young and A. R. Rickard (2012). "Development and chamber evaluation of the MCM v3.2 degradation scheme for beta-caryophyllene." Atmospheric Chemistry and Physics **12**(11): 5275-5308. DOI: 10.5194/acp-12-5275-2012.

Junkermann, W., J. Hacker, T. Lyons and U. Nair (2009). "Land use change suppresses precipitation." Atmospheric Chemistry and Physics **9**(17): 6531-6539.

Kanawade, V. P., B. T. Jobson, A. B. Guenther, M. E. Erupe, S. N. Pressley, S. N. Tripathi and S. H. Lee (2011). "Isoprene suppression of new particle formation in a mixed deciduous forest." Atmospheric Chemistry and Physics **11**(12): 6013-6027.

Karl, M., K. Tsigaridis, E. Vignati and F. Dentener (2009). "Formation of secondary organic aerosol from isoprene oxidation over Europe." Atmospheric Chemistry and Physics **9**(18): 7003-7030.

Kiendler-Scharr, A., J. Wildt, M. Dal Maso, T. Hohaus, E. Kleist, T. F. Mentel, R. Tillmann, R. Uerlings, U. Schurr and A. Wahner (2009). "New particle formation in forests inhibited by isoprene emissions." Nature **461**(7262): 381-384. DOI: 10.1038/nature08292.

Kiendler-Scharr, A., Q. Zhang, T. Hohaus, E. Kleist, A. Mensah, T. F. Mentel, C. Spindler, R. Uerlings, R. Tillmann and J. Wildt (2009). "Aerosol Mass Spectrometric Features of Biogenic SOA: Observations from a Plant Chamber and in Rural Atmospheric Environments." Environmental Science & Technology **43**(21): 8166-8172.

Kim, D. Y. and V. Ramanathan (2008). "Solar radiation budget and radiative forcing due to aerosols and clouds." Journal of Geophysical Research-Atmospheres **113**(D2).

Kim, S., A. Guenther, T. Karl and J. Greenberg (2011). "Contributions of primary and secondary biogenic VOC to total OH reactivity during CABINEX (Community Atmosphere-Biosphere INteractions Experiments)-09 field campaign." Atmospheric Chemistry and Physics **11**: 8613-8623.

Kleindienst, T. E., E. O. Edney, M. Lewandowski, J. H. Offenberg and M. Jaoui (2006). "Secondary organic carbon and aerosol yields from the irradiations of isoprene and alpha-pinene in the presence of NOx and SO2." Environmental Science & Technology **40**(12): 3807-3812.

Kleindienst, T. E., M. Lewandowski, J. H. Offenberg, M. Jaoui and E. O. Edney (2007). "Ozone-isoprene reaction: Re-examination of the formation of secondary organic aerosol." Geophysical Research Letters **34**(1).

Kleindienst, T. E., M. Lewandowski, J. H. Offenberg, M. Jaoui and E. O. Edney (2009). "The formation of secondary organic aerosol from the isoprene plus OH reaction in the absence of NOx." Atmospheric Chemistry and Physics **9**(17): 6541-6558.

Kokkola, H., P. Yli-Pirila, M. Vesterinen, H. Korhonen, H. Keskinen, S. Romakkaniemi, L. Hao, A. Kortelainen, J. Joutsensaari, D. R. Worsnop, A. Virtanen and K. E. J. Lehtinen (2014). "The role of low volatile organics on secondary organic aerosol formation." Atmospheric Chemistry and Physics **14**(3): 1689-1700. DOI: 10.5194/acp-14-1689-2014.

Kroll, J. H., N. L. Ng, S. M. Murphy, R. C. Flagan and J. H. Seinfeld (2005). "Secondary organic aerosol formation from isoprene photooxidation under high-NOx conditions." Geophysical Research Letters **32**(18). DOI: 10.1029/2005gl023637.

Kroll, J. H., N. L. Ng, S. M. Murphy, R. C. Flagan and J. H. Seinfeld (2006). "Secondary organic aerosol formation from isoprene photooxidation." Environmental Science & Technology **40**(6): 1869-1877. DOI: 10.1021/es0524301.

Lee, A., A. H. Goldstein, J. H. Kroll, N. L. Ng, V. Varutbangkul, R. C. Flagan and J. H. Seinfeld (2006a). "Gas-phase products and secondary aerosol yields from the photooxidation of 16 different terpenes." Journal of Geophysical Research-Atmospheres **111**(D17). DOI: 10.1029/2006jd007050.

Lee, A., A. H. Goldstein, M. D. Keywood, S. Gao, V. Varutbangkul, R. Bahreini, N. L. Ng, R. C. Flagan and J. H. Seinfeld (2006b). "Gas-phase products and secondary aerosol yields from the ozonolysis of ten different terpenes." Journal of Geophysical Research-Atmospheres **111**(D17). D07302, DOI:10.1029/2005JD006437.

Liggio, J., S. M. Li, J. R. Brook and C. Mihele (2007). "Direct polymerization of isoprene and α-pinene on acidic aerosols." Geophysical Research Letters, 34, L05814, 10.1029/2006gl028468.

Limbeck, A., M. Kulmala and H. Puxbaum (2003). "Secondary organic aerosol formation in the atmosphere via heterogeneous reaction of gaseous isoprene on acidic particles." Geophysical Research Letters, 30, 1996, 10.1029/2003gl017738.

Lin, P., J. Z. Yu, G. Engling and M. Kalberer (2012). "Organosulfates in Humic-like Substance Fraction Isolated from Aerosols at Seven Locations in East Asia: A Study by Ultra-High-Resolution Mass Spectrometry." Environmental Science & Technology, 46, 13118-13127, 10.1021/es303570v.

Lin, Y. H., Zhang, Z., Docherty, K. S., Zhang, H., Budisulistiorini, S. H., Rubitschun, C. L., Shaw, S. L., Knipping, E. M., Edgerton, E. S., Kleindienst, T. E., Gold, A., and Surratt, J. D.: Isoprene Epoxydiols as Precursors to Secondary Organic Aerosol Formation: Acid-Catalyzed Reactive Uptake Studies with Authentic Compounds, Environ. Sci. Technol., 46 (1), 250–258, doi: 10.1021/es202554c, 2012

Lin, Y.-H., H. Zhang, H. O. T. Pye, Z. Zhang, W. J. Marth, S. Park, M. Arashiro, T. Cui, S. H. Budisulistiorini, K. G. Sexton, W. Vizuete, Y. Xie, D. J. Luecken, I. R. Piletic, E. O. Edney, L. J. Bartolotti, A. Gold and J. D. Surratt (2013). "Epoxide as a precursor to secondary organic aerosol formation from isoprene photooxidation in the presence of nitrogen oxides." Proceedings of the National Academy of Sciences, 110, 6718-6723, 10.1073/pnas.1221150110.

Lin, Y. H., Knipping, E. M., Edgerton, E. S., Shaw, S. L., and Surratt, J. D.: Investigating the influences of SO_2 and NH_3 levels on isoprene-derived secondary organic aerosol formation using conditional sampling approaches, Atmos. Chem. Phys., 13, 8457-8470, doi: 10.5194/acp-13-8457-2013, 2013

MacKenzie, A. R., B. Langford, T. A. M. Pugh, N. Robinson, P. K. Misztal, D. E. Heard, J. D. Lee, A. C. Lewis, C. E. Jones, J. R. Hopkins, G. Phillips, P. S. Monks, A. Karunaharan, K. E. Hornsby, V. Nicolas-Perea, H. Coe, A. M. Gabey, M. W. Gallagher, L. K. Whalley, P. M. Edwards, M. J. Evans, D. Stone, T. Ingham, R. Commane, K. L. Furneaux, J. B. McQuaid, E. Nemitz, Y. K. Seng, D. Fowler, J. A. Pyle and C. N. Hewitt (2011). "The atmospheric chemistry of trace gases and particulate matter emitted by different land uses in Borneo." Philosophical Transactions of the Royal Society B-Biological Sciences **366**(1582): 3177-3195. DOI: 10.1098/rstb.2011.0053.

Matsunaga, A. and P. J. Ziemann (2010). "Gas-Wall Partitioning of Organic Compounds in a Teflon Film Chamber and Potential Effects on Reaction Product and

Aerosol Yield Measurements." Aerosol Science and Technology **44**(10): 881-892. DOI: 10.1080/02786826.2010.501044.

Mentel, T. F., E. Kleist, S. Andres, M. Dal Maso, T. Hohaus, A. Kiendler-Scharr, Y. Rudich, M. Springer, R. Tillmann, R. Uerlings, A. Wahner and J. Wildt (2013). "Secondary aerosol formation from stress-induced biogenic emissions and possible climate feedbacks." Atmospheric Chemistry and Physics **13**(17): 8755-8770. DOI: 10.5194/acp-13-8755-2013.

Mentel, T. F., J. Wildt, A. Kiendler-Scharr, E. Kleist, R. Tillmann, M. Dal Maso, R. Fisseha, T. Hohaus, H. Spahn, R. Uerlings, R. Wegener, P. T. Griffiths, E. Dinar, Y. Rudich and A. Wahner (2009). "Photochemical production of aerosols from real plant emissions." Atmospheric Chemistry and Physics **9**(13): 4387-4406.

Mercado, L. M., N. Bellouin, S. Sitch, O. Boucher, C. Huntingford, M. Wild and P. M. Cox (2009). "Impact of changes in diffuse radiation on the global land carbon sink." Nature **458**(7241): 1014-U1087.

Meyer, N. K., J. Duplissy, M. Gysel, A. Metzger, J. Dommen, E. Weingartner, M. R. Alfarra, A. S. H. Prevot, C. Fletcher, N. Good, G. McFiggans, A. M. Jonsson, M. Hallquist, U. Baltensperger and Z. D. Ristovski (2009). "Analysis of the hygroscopic and volatile properties of ammonium sulphate seeded and unseeded SOA particles." Atmospheric Chemistry and Physics **9**(2): 721-732.

Ng, N. L., J. H. Kroll, M. D. Keywood, R. Bahreini, V. Varutbangkul, R. C. Flagan, J. H. Seinfeld, A. Lee and A. H. Goldstein (2006). "Contribution of first- versus second-generation products to secondary organic aerosols formed in the oxidation of biogenic hydrocarbons." Environmental Science & Technology **40**(7): 2283-2297. DOI: 10.1021/es052269u.

Paulot, F., J. D. Crounse, H. G. Kjaergaard, A. Kurten, J. M. St Clair, J. H. Seinfeld and P. O. Wennberg (2009). "Unexpected Epoxide Formation in the Gas-Phase Photooxidation of Isoprene." Science **325**(5941): 730-733. DOI: 10.1126/science.1172910.

Paulson, S. E. and J. H. Seinfeld (1992). "DEVELOPMENT AND EVALUATION OF A PHOTOOXIDATION MECHANISM FOR ISOPRENE." Journal of Geophysical Research-Atmospheres **97**(D18): 20703-20715.

Riipinen, I., T. Yli-Juuti, J. R. Pierce, T. Petaja, D. R. Worsnop, M. Kulmala and N. M. Donahue (2012). "The contribution of organics to atmospheric nanoparticle growth." Nature Geosci **5**(7): 453-458.

Robinson, N. H., J. F. Hamilton, J. D. Allan, B. Langford, D. E. Oram, Q. Chen, K. Docherty, D. K. Farmer, J. L. Jimenez, M. W. Ward, C. N. Hewitt, M. H. Barley, M. E. Jenkin, A. R. Rickard, S. T. Martin, G. McFiggans and H. Coe (2010). "Evidence for a significant proportion of Secondary Organic Aerosol from isoprene above a maritime tropical forest." Atmos. Chem. Phys. Discuss. **10**(11): 25545-25576.

Robinson, N. H., J. F. Hamilton, J. D. Allan, B. Langford, D. E. Oram, Q. Chen, K. Docherty, D. K. Farmer, J. L. Jimenez, M. W. Ward, C. N. Hewitt, M. H. Barley, M. E. Jenkin, A. R. Rickard, S. T. Martin, G. McFiggans and H. Coe (2011). "Evidence for a significant proportion of Secondary Organic Aerosol from isoprene above a maritime tropical forest." Atmospheric Chemistry and Physics **11**(3): 1039-1050. DOI: 10.5194/acp-11-1039-2011.

Rollins, A. W., A. Kiendler-Scharr, J. L. Fry, T. Brauers, S. S. Brown, H. P. Dorn, W. P. Dube, H. Fuchs, A. Mensah, T. F. Mentel, F. Rohrer, R. Tillmann, R. Wegener, P. J. Wooldridge and R. C. Cohen (2009). "Isoprene oxidation by nitrate radical: alkyl nitrate and secondary organic aerosol yields." Atmospheric Chemistry and Physics **9**(18): 6685-6703.

Ruppert, L. and K. H. Becker (2000). "A product study of the OH radical-initiated oxidation of isoprene: formation of C-5-unsaturated diols." Atmospheric Environment **34**(10): 1529-1542.

Sillman, S. (1999). "The relation between ozone, NOx and hydrocarbons in urban and polluted rural environments." Atmospheric Environment **33**(12): 1821-1845.

Sprengnether, M., K. L. Demerjian, N. M. Donahue and J. G. Anderson (2002). "Product analysis of the OH oxidation of isoprene and 1,3-butadiene in the presence of NO." Journal of Geophysical Research-Atmospheres **107**(D15). DOI: 10.1029/2001jd000716.

Stevens, B. and G. Feingold (2009). "Untangling aerosol effects on clouds and precipitation in a buffered system." Nature **461**(7264): 607-613.

Surratt, J. D., A. W. H. Chan, N. C. Eddingsaas, M. Chan, C. L. Loza, A. J. Kwan, S. P. Hersey, R. C. Flagan, P. O. Wennberg and J. H. Seinfeld (2010). "Reactive intermediates revealed in secondary organic aerosol formation from isoprene." Proceedings of the National Academy of Sciences **107**(15): 6640-6645. DOI: 10.1073/pnas.0911114107.

Surratt, J. D., M. Lewandowski, J. H. Offenberg, M. Jaoui, T. E. Kleindienst, E. O. Edney and J. H. Seinfeld (2007). "Effect of Acidity on Secondary Organic Aerosol Formation from Isoprene." Environmental Science & Technology **41**(15): 5363-5369.

Surratt, J. D., S. M. Murphy, J. H. Kroll, N. L. Ng, L. Hildebrandt, A. Sorooshian, R. Szmigielski, R. Vermeylen, W. Maenhaut, M. Claeys, R. C. Flagan and J. H. Seinfeld (2006). "Chemical composition of secondary organic aerosol formed from the photooxidation of isoprene." Journal of Physical Chemistry A **110**(31): 9665-9690. DOI: 10.1021/jp061734m.

Surratt, J. D., S. M. Murphy, J. H. Kroll, N. L. Ng, L. Hildebrandt, A. Sorooshian, R. Szmigielski, R. Vermeylen, W. Maenhaut, M. Claeys, R. C. Flagan and J. H. Seinfeld (2006). "Chemical Composition of Secondary Organic Aerosol Formed from the Photooxidation of Isoprene." The Journal of Physical Chemistry A **110**(31): 9665-9690.

Surratt, J. D., A. W. H. Chan, N. C. Eddingsaas, M. Chan, C. L. Loza, A. J. Kwan, S. P. Hersey, R. C. Flagan, P. O. Wennberg and J. H. Seinfeld (2010). "Reactive intermediates revealed in secondary organic aerosol formation from isoprene." Proceedings of the National Academy of Sciences, 107, 6640-6645, 10.1073/pnas.0911114107, 2010.

Tuazon, E. C. and R. Atkinson (1990). "A PRODUCT STUDY OF THE GAS-PHASE REACTION OF ISOPRENE WITH THE OH RADICAL IN THE PRESENCE OF NOX." International Journal of Chemical Kinetics **22**(12): 1221-1236. DOI: 10.1002/kin.550221202.

van Donkelaar, A., R. V. Martin, R. J. Park, C. L. Heald, T. M. Fu, H. Liao and A. Guenther (2007). "Model evidence for a significant source of secondary organic aerosol from isoprene." Atmospheric Environment **41**(6): 1267-1274. DOI: 10.1016/j.atmosenv.2006.09.051.

VanReken, T. M., J. P. Greenberg, P. C. Harley, A. B. Guenther and J. N. Smith (2006). "Direct measurement of particle formation and growth from the oxidation of biogenic emissions." Atmospheric Chemistry and Physics **6**: 4403-4413.

Verheggen, B. and M. Mozurkewich (2006). “An inverse modeling procedure to determine particle growth and nucleation rates from measured aerosol size distributions.” Atmos. Chem. Phys., 6, 2927-2942, doi:10.5194/acp-6-2927-2006.

Virtanen, A., J. Joutsensaari, T. Koop, J. Kannosto, P. Yli-Pirila, J. Leskinen, J. M. Makela, J. K. Holopainen, U. Poschl, M. Kulmala, D. R. Worsnop and A. Laaksonen (2010). "An amorphous solid state of biogenic secondary organic aerosol particles." Nature **467**(7317): 824-827.

Wang, W., G. Vas, R. Dommisse, K. Loones and M. Claeys (2004). "Fragmentation study of diastereoisomeric 2-methyltetrols, oxidation products of isoprene, as their trimethylsilyl ethers, using gas chromatography/ion trap mass spectrometry." Rapid Communications in Mass Spectrometry **18**(16): 1787-1797. DOI: 10.1002/rcm.1553.

Wyche, K. P., R. S. Blake, A. M. Ellis, P. S. Monks, T. Brauers, R. Koppmann and E. C. Apel (2007). "Technical note: Performance of Chemical Ionization Reaction Time-of-Flight Mass Spectrometry (CIR-TOF-MS) for the measurement of atmospherically significant oxygenated volatile organic compounds." Atmospheric Chemistry and Physics **7**: 609-620.

Wyche, K. P., et al. (2014) "Mapping organic reactivity during secondary organic aerosol formation". **In Preparation**.

Zhang, Q., J. L. Jimenez, M. R. Canagaratna, J. D. Allan, H. Coe, I. Ulbrich, M. R. Alfarra, A. Takami, A. M. Middlebrook, Y. L. Sun, K. Dzepina, E. Dunlea, K. Docherty, P. F. DeCarlo, D. Salcedo, T. Onasch, J. T. Jayne, T. Miyoshi, A. Shimono, S. Hatakeyama, N. Takegawa, Y. Kondo, J. Schneider, F. Drewnick, S. Borrmann, S. Weimer, K. Demerjian, P. Williams, K. Bower, R. Bahreini, L. Cottrell, R. J. Griffin, J. Rautiainen, J. Y. Sun, Y. M. Zhang and D. R. Worsnop (2007). "Ubiquity and dominance of oxygenated species in organic aerosols in anthropogenically-influenced Northern Hemisphere midlatitudes." Geophysical Research Letters **34**(13). DOI: 10.1029/2007gl029979.

Zhao, J., R. Zhang, E. C. Fortner and S. W. North (2004). "Quantification of hydroxycarbonyls from OH-isoprene reactions." Journal of the American Chemical Society **126**: 2686-2687.

Tables

Table 1: List of experiments conducted and their general parameters

Date	Tree Species	Initial NO_x / ppbV	VOC/NO_x	Relative Humidity / %	Pre-existing Seed
22/06/09	*Ficus benjamina*	3	4.2	79	None
23/06/09	*Ficus benjamina*	6	2.7	75	None
25/06/09	*Ficus benjamina*	2	6.3	65	Sulphate
29/06/09	*Ficus cyathistipula*	2	9.4	71	None
30/06/09	*Ficus cyathistipula*	2	7.8	75	Sulphate
02/07/09	*Ficus cyathistipula*	3	5.6	78	Sulphate
06/07/09	*Betula pendula*	3	5.6	84	None
07/07/09	*Betula pendula*	3	5.5	73	Sulphate
09/07/09	*Betula pendula*	2	1.5	70	Sulphate
10/07/09	*Betula pendula* + 36 ppbV isoprene	2	5.5	70	Sulphate
13/07/09	*Ficus benjamina*	2	-[1]	87	Sulphate
15/07/09	*Ficus benjamina*	3	-[1]	89	Sulphate

16/07/09	*Ficus benjamina* + 4.5 ppbV limonene	2	-[1]	85	None

Notes:

1. No quantified VOC data available

Table 2: GC-MS identification of the biogenic VOC present in the plant chamber air immediately before RC filling began. Quantification of isoprene, total monoterpenes and total sesquiterpenes was carried out using PTR-MS and CIRMS (see Figures 2 and 5).

Experiment	Compounds detected by GC-MS (abundance ppbV) (trace = <0.1 ppb)			
	Isoprene	Monoterpenes (and related)	Sesquiterpenes	Other
B. Pendula	Yes (0.25-1.19)	α-pinene (0.31 – 1.08) β-pinene (0.74 – 7.19) ocimene (trace – 1.22) Δ3-carene (1.89 – 4.94) γ-terpinene (trace) 2, 4, 6-octatriene,2,6-dimethyl (trace) 4,7-methano-1H-indene, octahydro (trace)	β-caryophyllene (0.15 – 0.22) α-farnesene (0.14) α-caryophyllene (0.59 – 0.92) α-copaene (trace) aromadendrene (0.45-0.51) α-cedrene (trace) α-pyronene (trace)	acetaldehyde (trace) caryophyllene-epoxide (trace) nerolidol (trace) linalool (trace)

F. Benjamina	Yes (38.49)	α-pinene (trace) limonene (trace) sabinene (trace) linalool (trace)	α-cubebene (trace)	acetaldehyde (trace) benzoquinone (trace) pyridine (trace) methyl salicate (trace) decanal (trace)
F. Cyathistipula	Yes (75.08)	α-pinene (trace) β-pinene (trace) limonene (trace)	β-caryophyllene (trace)	acetic acid (trace)
Mixed canopy *F. Benjamina* *F. Cyathistipula* *C. Millis*	Yes	α-pinene (0.37) camphene (0.11) limonene (0.42) ocimene (trace)	None detected	*p*-dichlorobenzene methyl salicate

Table 3: Yields of isoprene oxidation products compared to literature values. Yields are an average from all *Ficus* experiments (seeded and unseeded) (n = 4) calculated at 4 hours after lights on (HALO). Yield is based on the calculated relationship between the amount of isoprene reacted and the oxidation product in question.

Isoprene	Hydro-peroxides[1]	MVK +MACR	Hydroxy-acetone	Form-aldehyde	Source
1	0.33	0.26	0.07		Williams et al 1999
1	0.05	0.36	0.05		Williams et al 2001 (NO_x present)
1		0.33		0.67	Zang et al 2002
1		0.46 – 0.60		0.86 – 0.96	Niki et al 1983 Kamens et al 1982
1	0.18	0.25			Surratt et al 2010 NO_x present NO_x absent
1		0.27			Kleindienst et al 2009
1	0.01 –	0.17 – 0.36	0 – 0.02	0.02 – 0.07	This study

Isoprene	Hydroperoxides[1]	MVK +MACR	Hydroxyacetone	Formaldehyde	Source
	0.03				

Notes:

1. Sum of isoprene epoxide (IEPOX) and isoprene hydroperoxide (ISOPOOH)

Figures

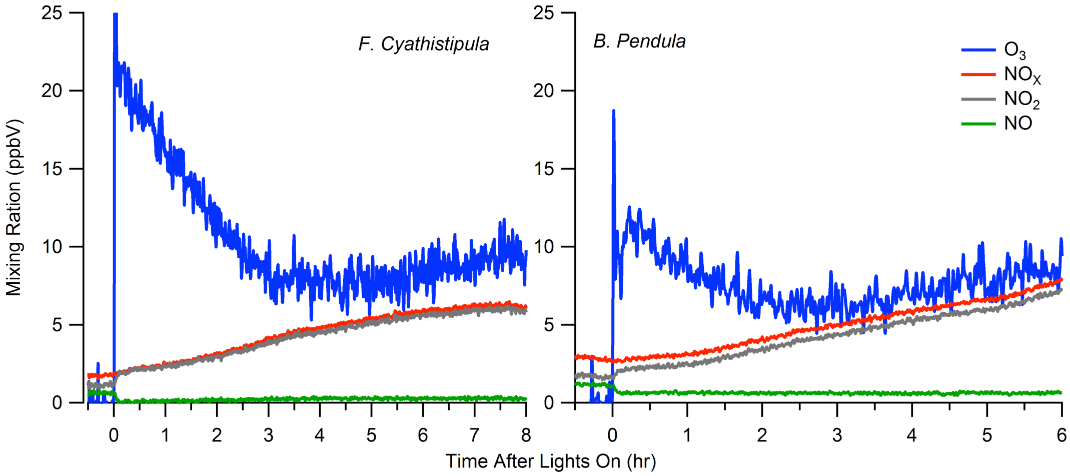

Figure 1**:** Temporal evolution of NO, NO_2, NO_x and O_3 during typical *Ficus Cyathistipula* (a) and *Betula pendula* (b) experiments (25/06/09 and 07/07/09, respectively).

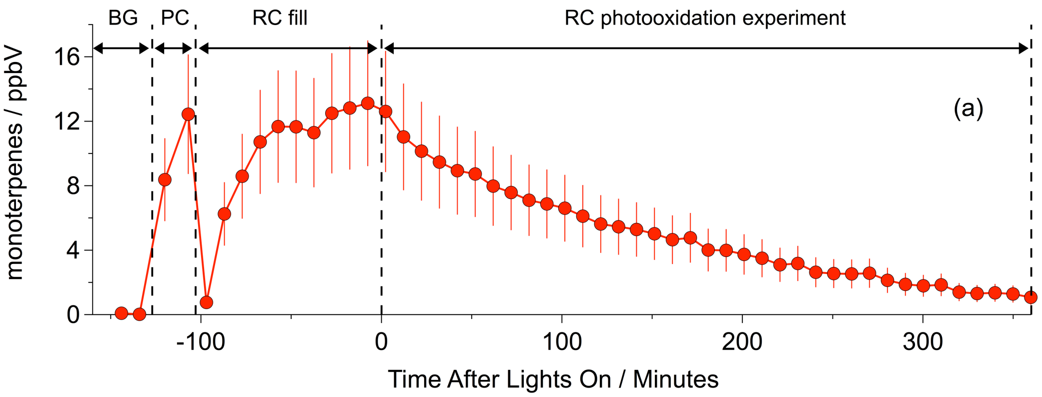

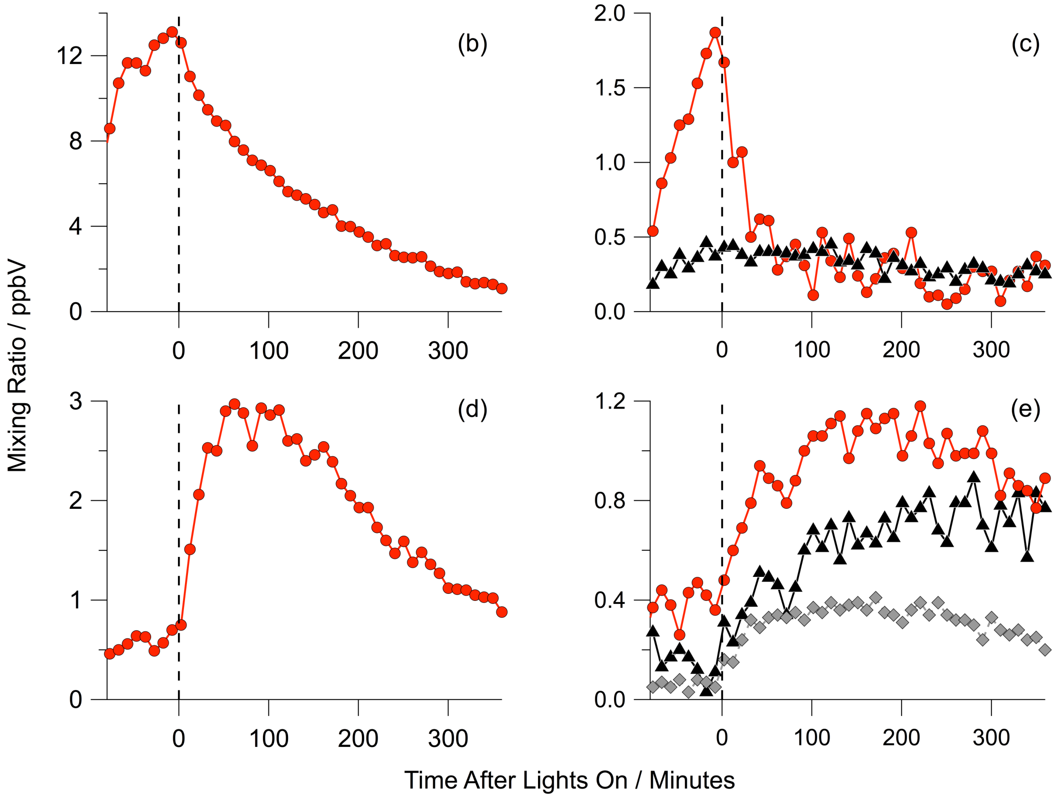

Figure 2: Temporal evolution of a series of isoprenoid “precursor” compounds and their oxidation products, as observed in the main reaction chamber during an example *Betula pendula* experiment (07/0709). The top panel (a) shows the entire experiment process in terms of monoterpene evolution, from background (BG) and plant chamber (PC) measurements, to reaction chamber (RC) fill and the main photooxidation experiment within the reaction chamber. Figure (b) shows monoterpene evolution, (c) shows sequiterpenes (red circles and lines) and camphore (black triangles and lines), (d) $\Sigma(I_{111}, I_{93})$ and (e) the primary ketone (*m/z* 139) (red circles and lines), primary keto-aldehyde (*m/z* 107 + 151 + 169) (black triangles and lines) and MVK + MACR (*m/z* 71) (grey diamonds and dashed line).

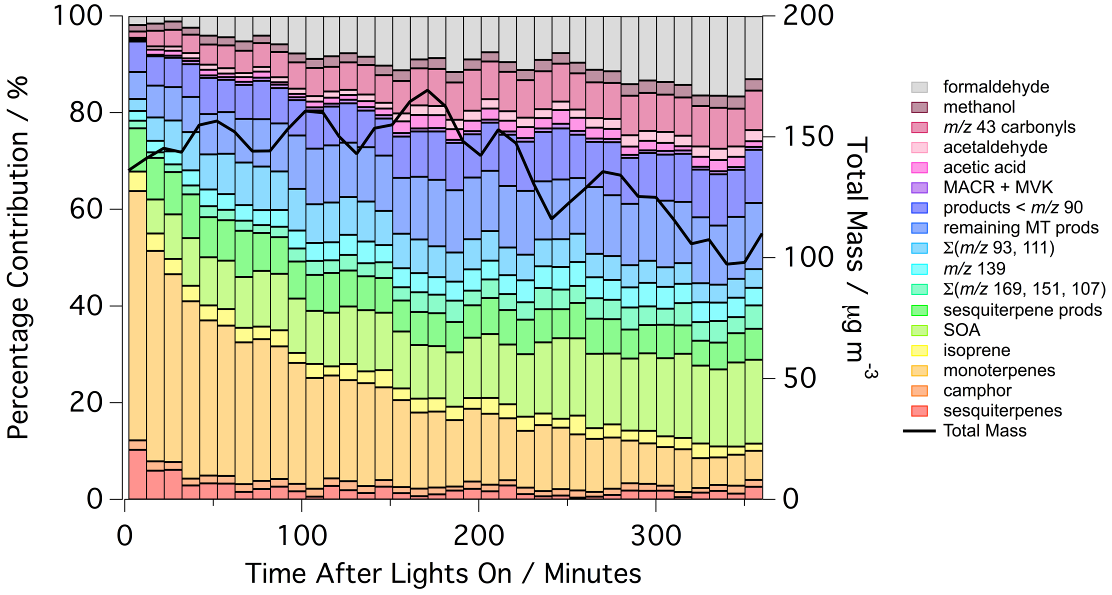

Figure 3: Evolution of measured mass through the *Betula pendula* system (7 July 2009), showing the relative contribution of precursor compounds, oxidation products and SOA mass to total measured mass, with time (coloured bars, left axis) and total measured mass (i.e. ΣVOCs + SOA) with time (black line, right axis). Note: ammonium sulphate seed mass removed from the SOA mass concentration.

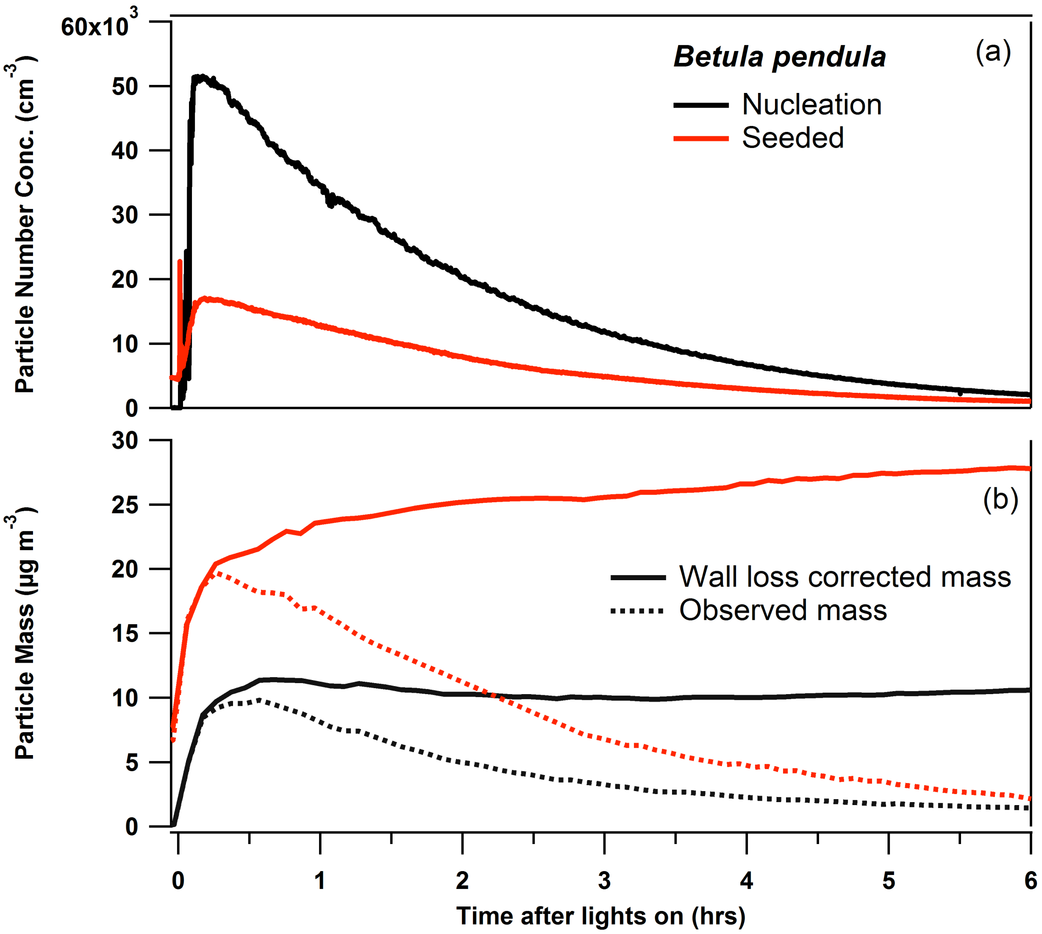

Figure 4: Particle number and mass concentrations measured during nucleation (06/07/09) and ammonium sulphate seeded (07/07/09) *Betula pendula* experiments (a). In the bottom panel (b), both the measured (dashed lines) and the wall loss corrected (solid lines) mass concentrations are shown.

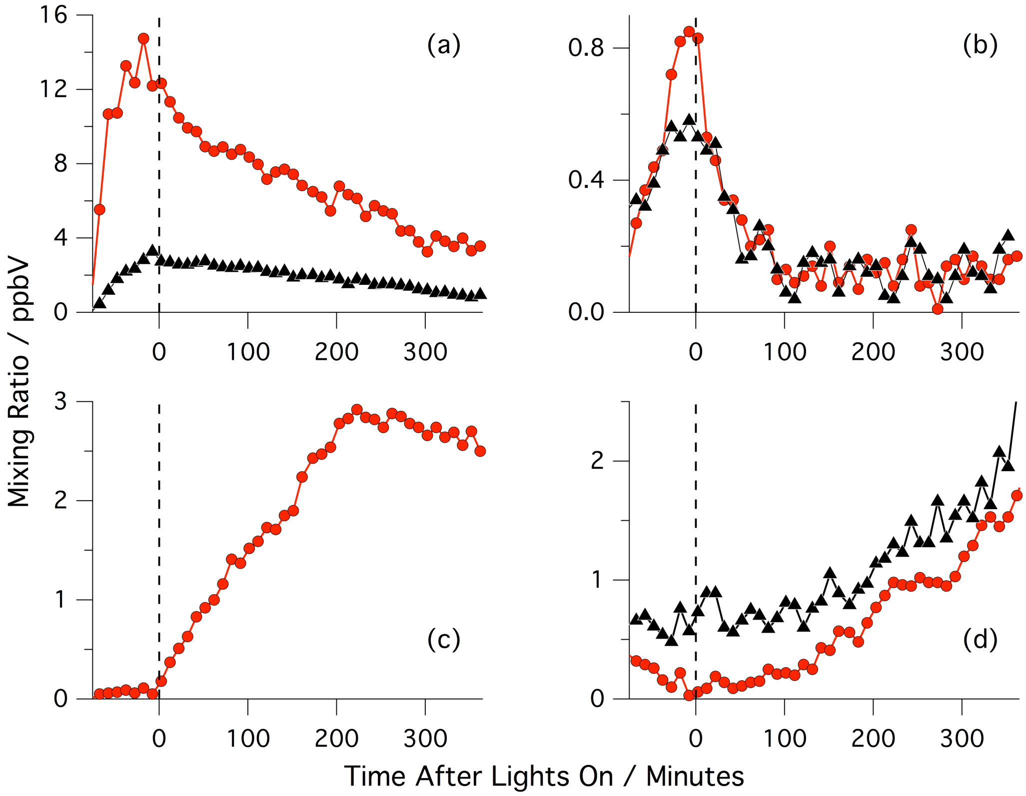

Figure 5: Temporal evolution of a series of isoprenoid "precursor" compounds and their oxidation products, as observed in the main reaction chamber during an example *Ficus benjamina* experiment (23/06/09). Panel (a) shows isoprene (red circles and lines) and camphore (black triangles and lines) evolution, (b) shows monoterpenes (red circles and lines) and sesquiterpenes (black triangles and lines), (c) MVK + MACR (*m/z* 71) and (d) Σ(monoterpene products) (black triangles and lines) and Σ(non MVK+MACR isoprene products) (red circles and lines)

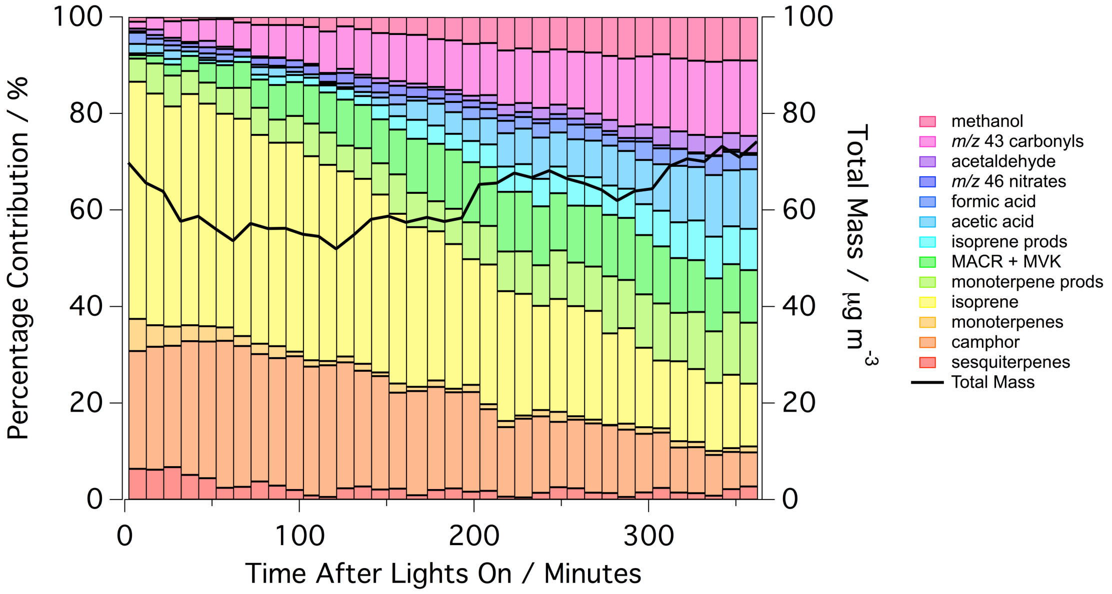

Figure 6: Evolution of measured mass through the *Ficus benjamina* system (23 June 2009), showing the relative contribution of precursor compounds and oxidation products to total measured mass, with time (coloured bars, left axis) and total measured mass (i.e. ΣVOCs + SOA) with time (black line, right axis).

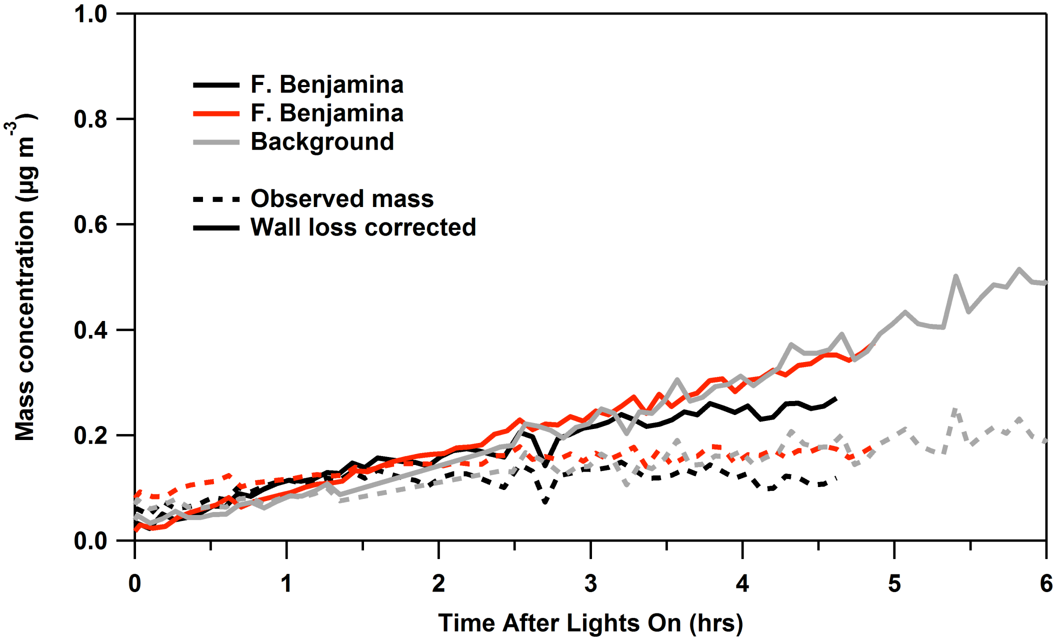

Figure 7: Observed and wall loss corrected particle mass concentrations during un-seeded *Ficus benjamina* (22/06/09, 23/06/09) and chamber background (26/06/09) experiments. The reaction chamber was filled with plant chamber air over a period of 1 – 1.5 hours. Chamber filling was carried out in the dark. Ozone was added immediately prior to lights on. Time begins at the point at which the reaction chamber was illuminated, then increments in hours after lights on.

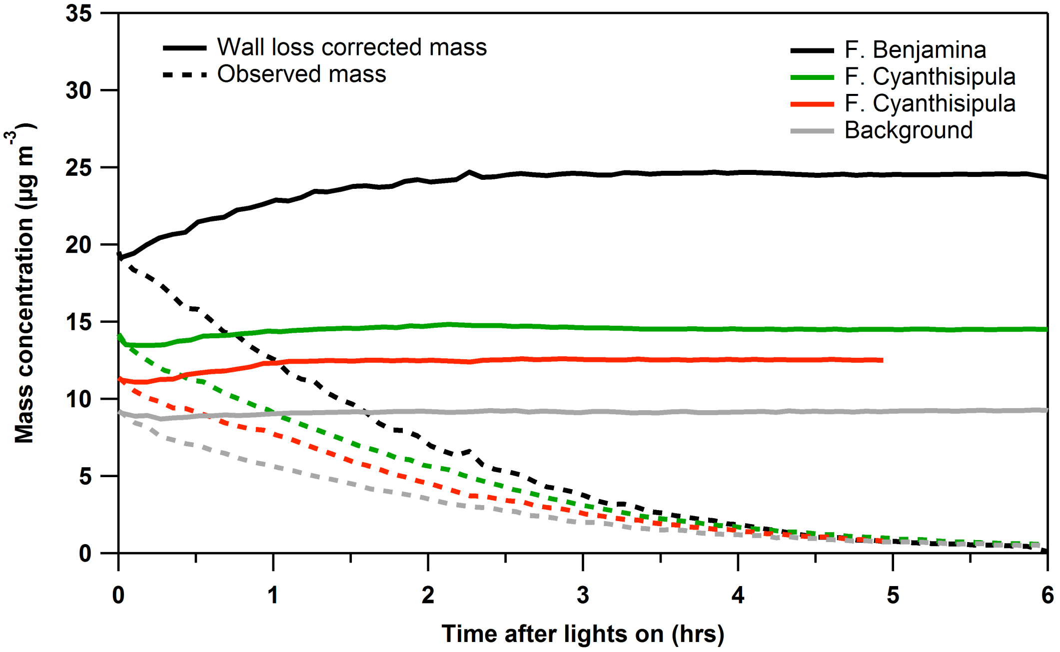

Figure 8: Observed and wall loss corrected particle mass concentrations during ammonium sulphate seeded *Ficus benjamina* (15/07/09)*, Ficus cyathistipula* (30/06/09, 02/07/09) and chamber background (03/07/09) experiments. Ozone and ammonium sulphate seed were added immediately prior to lights on.

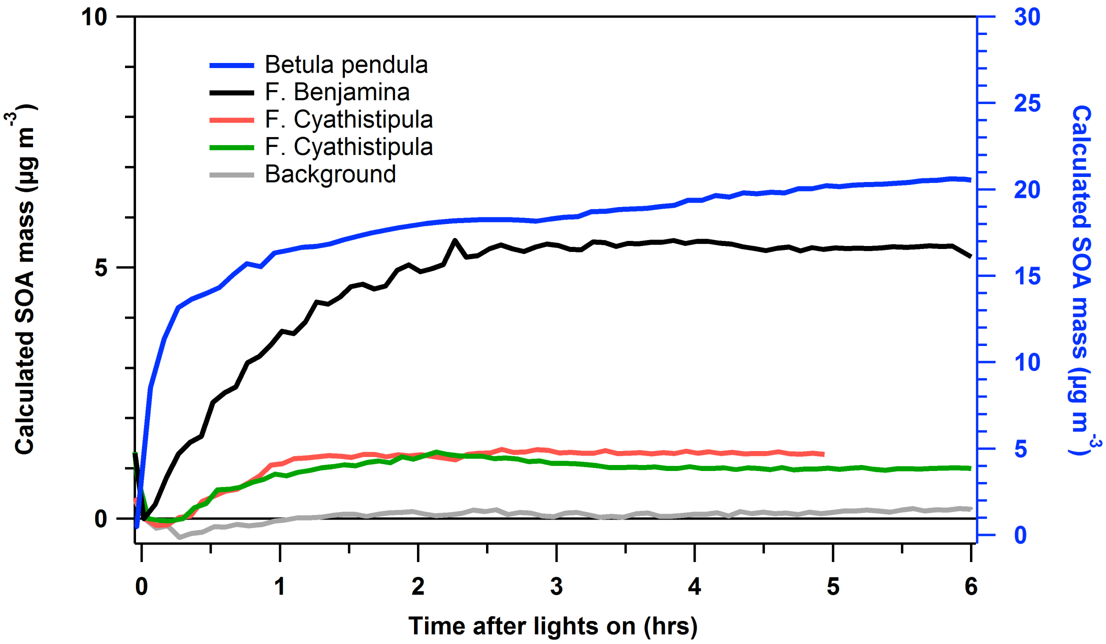

Figure 9: Calculated SOA mass concentrations during ammonium sulphate seeded experiments for *Betula pendula* (07/07/09), *Ficus benjamina* (15/07/09) and *Ficus cyathistipula* (30/06/09, 02/07/09). See text for details.

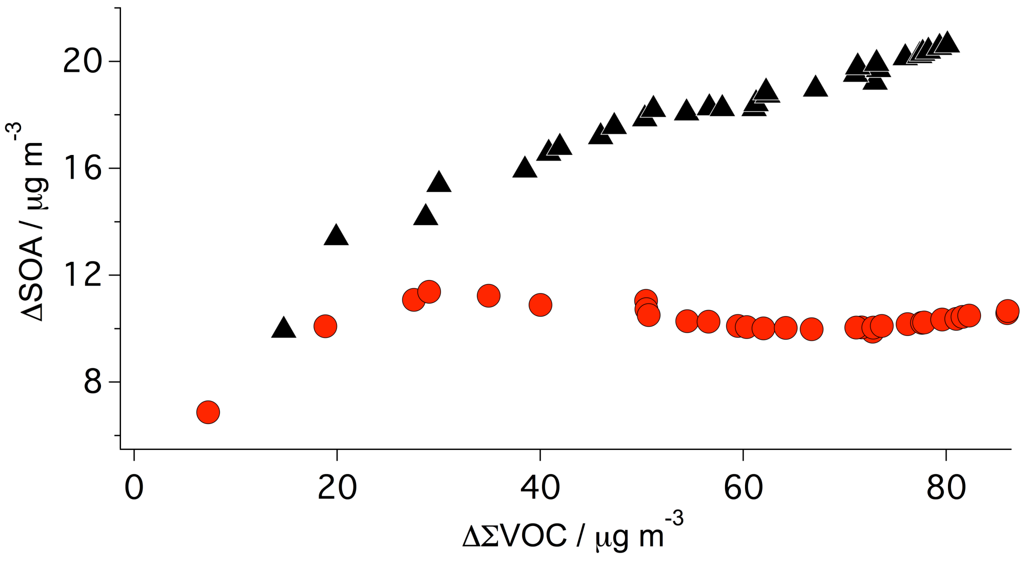

Figure 10: Time dependent growth curves for two typical *Betula pendula* experiments (red circles- nucleation experiment on 06/07/09 and black triangles- ammonium sulphate seeded experiment on 07/07/09), showing SOA growth behaviour with respect to consumption of the VOC precursors.

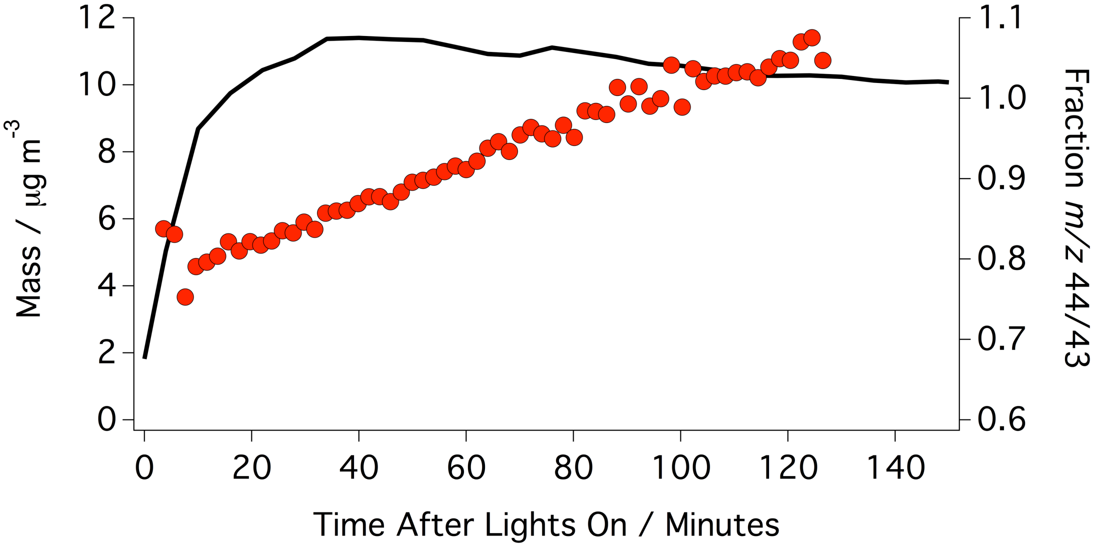

Figure 11: Temporal evolution of the *m/z* 44/43 ratio (red circles) during a typical *Betula pendula* experiment (06/07/09) and wall loss corrected SOA mass (black line); demonstrating the increase in oxygenated content of the SOA as the air matrix begins to age.

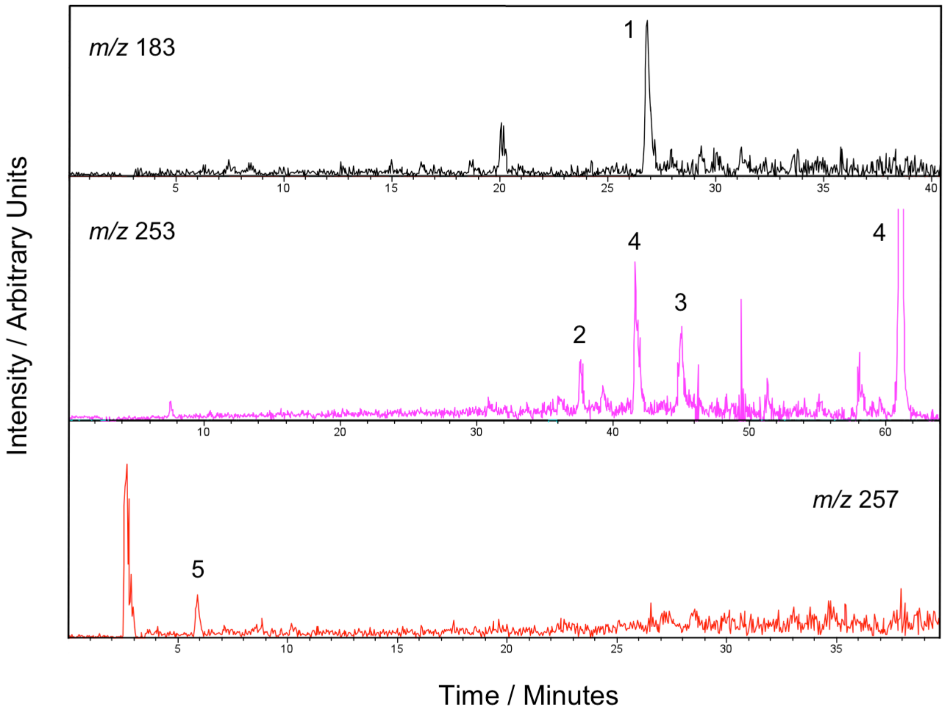

Figure 12: LC-MS^2 selected ion chromatograms derived from the off-line analysis of SOA collected on filters at the conclusion of a typical *Betula pendula* experiment (07/07/2009). Notes: Upper; *m/z* 183 = MW 184, 1 = cis-pinonic acid. Middle; *m/z* 253 = MW 254, 2 = β-nocaryophyllonic acid, 3 = β-caryophyllinic acid, 4 = similar to sesquiterpene SOA. Lower; *m/z* 257 = MW 118 [2*[M-H] + Na]$^-$, also seen in myrcene SOA, with same MS^2 spectra.